CA2 neurons show abnormal responses to social stimuli in a rat model of Fragile X syndrome

Margaret M. Donahue[#1,2,3], Emma Robson[#2,3], Alyssa M. Marron[1,2,3,4], Edel J. Fernandez[2,3], Misty Hill[2,3], Alexandra J. Mably[2,3], John B. Trimper[2,3], Darrin H. Brager[2,4,5], Laura Lee Colgin[1,2,3]

[#]Contributed equally
[1]Interdisciplinary Neuroscience Program, The University of Texas at Austin, Austin, Texas, 78712
[2]Center for Learning and Memory, The University of Texas at Austin, Austin, Texas, 78712
[3]Department of Neuroscience, The University of Texas at Austin, Austin, Texas, 78712
[4]School of Life Sciences, University of Nevada at Las Vegas, Las Vegas, Nevada, 92154
[5]Interdisciplinary Neuroscience Program, University of Nevada at Las Vegas, Las Vegas, Nevada, 92154

Abbreviated title: CA2 neuronal responses in a Fragile X rat model

Corresponding author: Laura Lee Colgin, colgin@mail.clm.utexas.edu

Number of pages: 42; **Number of figures**: 8 main figures and 2 supplemental figures; **Number of tables**: 2

Number of words: Abstract: 138; Significance statement: 93; Introduction: 630; Discussion: 1350

Conflict of interest: The authors declare no competing financial interests.

Acknowledgments: This research was supported by the Department of Defense CDMRP award W81XWH1810314 (to L.L.C.), Brain and Behavior Research Foundation (BBRF) Distinguished Investigator Grant 32221 (to L.L.C.), and National Institutes of Health awards R56MH125655 (to D.H.B. and L.L.C), R01MH131317 (to D.H.B. and L.L.C.), and F31MH127933 (to M.M.D.). The authors thank Isabella Lee, Ayomide Akinsooto, and Sirisha Dhavala for technical assistance and Chenguang Zheng for providing MATLAB code for some of the analyses. We also thank Dr. Moses V. Chao and Dr. Robert C. Froemke from New York University School of Medicine for generously providing the OXTR-2 antibody used in this study. The authors acknowledge the Texas Advanced Computing Center (TACC) at The University of Texas at Austin for providing data storage resources that have contributed to the research described within this article. URL: http://www.tacc.utexas.edu

Author contributions:
M.M.D. performed research, analyzed data, and wrote the paper; E.R. designed research, performed research, analyzed data, and wrote the paper; A.M.M. performed research; E.J.F. analyzed data; M.H. performed research and analyzed data; A.J.M. designed research, performed research, and analyzed data; J.B.T. performed research; D.H.B. designed research, performed research, and wrote the paper; L.L.C. designed research, analyzed data, and wrote the paper.

Abstract

Fragile X Syndrome (FXS) is a neurodevelopmental disorder that is highly comorbid with autism spectrum disorders and can cause abnormal social behaviors. The CA2 subregion of the hippocampus is essential for social memory processing and social recognition. A social interaction induces changes in CA2 neuronal firing; however, it is unknown whether these changes are impaired in FXS models. Here, we examined CA2 activity in a rat model of Fragile X Syndrome (*Fmr1* knockout rats). In *Fmr1* knockout rats, we observed impaired CA2 cell responses to social stimuli, despite similar social behaviors. Further, in CA2 of *Fmr1* knockout rats, we found reduced expression of oxytocin receptors and impaired whole cell responses to oxytocin. Together, these results raise the possibility that abnormal CA2 activity contributes to impaired social behavior in FXS and may suggest novel treatment targets for FXS patients.

Significance statement

Fragile X Syndrome (FXS) is a neurodevelopmental disorder that can result in abnormal social behaviors, including social avoidance. Activity in the CA2 subregion of the hippocampus is believed to support social recognition and social cognition. Yet, the extent to which the CA2 subregion of the hippocampus is affected by FXS is poorly understood. In this study, we identified specific impairments in CA2 neuronal responses to social stimuli in a rat model of FXS. Further, we provide evidence suggesting that CA2 responses to oxytocin, a neuropeptide released during social interactions, are abnormal in FXS.

24 **Introduction**

25

26 Fragile X Syndrome (FXS) is a neurodevelopmental disorder that is highly co-morbid with
27 autism spectrum disorders. Patients with FXS often display abnormal social behaviors, including
28 social avoidance (Kau et al., 2004; Kaufmann et al., 2004; Lesniak-Karpiak et al., 2003;
29 Merenstein et al., 1996; Williams et al., 2014). FXS is caused by a deficit in the function of
30 Fragile X Messenger Ribonucleoprotein (FMRP). FMRP is the product of the *Fmr1* gene, which
31 is located on the X chromosome. FXS is caused by hypermethylation and transcriptional
32 silencing of the *Fmr1* gene (Pieretti et al., 1991; Verkerk et al., 1991), leading to a complete lack
33 of FMRP production. FMRP is an RNA-binding protein (Ashley et al., 1993; Siomi et al., 1993)
34 believed to regulate translation and protein synthesis in neurons (Jin & Warren, 2000; Richter &
35 Zhao, 2021). Mouse and rat models of FXS (hereafter termed “FXS mice” and “FXS rats”,
36 respectively) have been developed by knocking out the homologous *fmr1* gene in these species
37 (Bakker et al., 1994; Hamilton et al., 2014; Mientjes et al., 2006; Tian et al., 2017).

38

39 Social behavior deficits have been observed in FXS rodent models. FXS mice display more
40 anxiety-like behaviors during social interactions (McNaughton et al., 2008; Spencer et al., 2005)
41 and lower levels of social interaction (Liu & Smith, 2009; McNaughton et al., 2008; Mineur et al.,
42 2006; Oddi et al., 2014) than wild-type (WT) mice. In addition, FXS mice and rats may be
43 deficient in distinguishing between positive and negative (McNaughton et al., 2008), or familiar
44 and novel (Tian et al., 2017), social interactions.

45

46 The CA2 region of the hippocampus is essential for social recognition (Oliva, 2022). Inactivating
47 CA2 pyramidal cells impairs social memory and recognition (Hitti & Siegelbaum, 2014; Meira et
48 al., 2018; Oliva et al., 2020; Stevenson & Caldwell, 2014). CA2, like all subregions of the rodent

49 hippocampus, contains place cells, neurons that have spatial receptive fields called place fields
50 (O'Keefe & Dostrovsky 1971). Place cells often alter their firing patterns in response to changes
51 in sensory or cognitive input in a process referred to as “remapping” (Colgin et al., 2008). During
52 “global” remapping, place fields may appear, disappear, or change location. During “rate”
53 remapping, place fields do not move, but cells’ in-field firing rates change. Previous research
54 has shown that the introduction of a social stimulus to a familiar environment induces global
55 remapping in CA2 place cells (Alexander et al., 2016; Robson et al., 2025). Furthermore, this
56 process appears to be driven by the olfactory content of social experiences (Robson et al.,
57 2025). CA2 place cell responses to social stimuli may reflect a cellular mechanism underlying
58 CA2’s contributions to social memory.
59
60 In this study, we recorded CA2 place cells in FXS rats and WT control rats freely exploring an
61 open field arena. We analyzed changes in CA2 place cell firing patterns when stimuli with a
62 social olfactory component were added to the arena. We found that the presentation of social
63 odors was associated with global remapping in CA2 place cells in WT rats but not FXS rats.
64 Receptors for oxytocin, a neuropeptide that regulates social behaviors and social memory
65 (Froemke & Young 2021), are prominently expressed in CA2 (Mitre et al. 2016), and
66 administration of an oxytocin receptor agonist potentiated excitatory postsynaptic currents
67 (EPSCs) in CA2 neurons (Pagani et al. 2015). Thus, we hypothesized that abnormal CA2
68 neuronal responses to oxytocin contribute to deficient CA2 place cell remapping to social stimuli
69 in FXS rats. In accord with this hypothesis, we observed reduced oxytocin receptor expression
70 and impaired depolarizing responses to oxytocin in CA2 neurons in FXS rats. Together, these
71 results suggest that CA2 cellular responses involved in social information processing may be
72 impaired in FXS. The results also point to potential mechanisms that may contribute to
73 abnormal social behaviors in FXS.

74

75 **Materials & Methods**

76

77 *Subjects*

78

79 The FXS rats used in this study were *fmr1*-knockout rats on a Sprague-Dawley background
80 (SD-*Fmr1*-/null^{tm1Sage}). Control rats used in this study were WT Sprague-Dawley rats. Both WT
81 and FXS rats were obtained from Inotiv. As FXS is an X chromosome-linked disorder, the
82 prevalence of FXS is higher in males, and symptoms tend to be more severe in male patients
83 than female patients. Therefore, we chose to use male rats. All experiments were conducted
84 according to the guidelines of the United States National Institutes of Health Guide for the Care
85 and Use of Laboratory Animals. *In vivo* and *in vitro* studies were conducted under protocols
86 approved by the Institutional Animal Care and Use Committees at the University of Texas at
87 Austin and the University of Nevada at Las Vegas, respectively.

88

89 *Subjects for CA2 place cell recordings and open field exploration.* CA2 place cell recordings in
90 this study were collected from twelve male rats. Six were WT control rats, and six were FXS
91 rats. The six WT rats used in the *in vivo* portion of this study were included in one previously
92 published study (Robson et al., 2025); one of the WT rats and three of the FXS rats were
93 included in another previously published study (Donahue, Robson, & Colgin 2025). Rats were
94 between the ages of 3 and 10 months old at the time of surgery. Before surgery, rats were
95 double or tripled housed with littermates in same-genotype cages. Following surgery, rats were
96 housed singly in custom-built acrylic cages (40 cm x 40 cm x 40 cm) to prevent damage to
97 implants. Enrichment material (i.e., paper towel rolls, wooden blocks, etc.) was added to the
98 cages, and rats were housed directly next to the cage of their former cage mates throughout

99 behavioral neurophysiology data collection. Rats were maintained on a reverse light cycle (light:
100 8 p.m. – 8 a.m.), and all behavioral neurophysiology experiments were performed during the
101 dark cycle. When necessary to encourage open field exploration, rats were temporarily placed
102 on a food deprivation protocol. Five WT rats and one FXS rat experienced temporary food
103 deprivation. With the provided food and treats consumed during open field exploration (see
104 "*Open field behavioral task*" section below), rats on food deprivation maintained at least 97% of
105 their free-feeding body weight.
106
107 After experiments had concluded, tissue (~1-2 mm) was collected from anesthetized rats
108 immediately prior to terminal perfusion. Tissue samples were then stored at -20°C and sent to
109 Transnettyx Inc. to verify rats' genotypes.
110
111 *Subjects for olfactory habituation/dishabituation testing.* Thirty-six rats (18 WT rats and 18 FXS
112 rats) were included in the olfactory habituation/dishabituation behavioral task in this study. Two
113 of the WT rats and four of the FXS rats were the same rats used for recording CA2 place cells.
114 Rats who were included in both olfactory habituation/dishabituation tests and CA2 place cell
115 recording studies completed olfactory testing prior to undergoing implantation surgery and CA2
116 data collection. All olfactory habituation/dishabituation testing was performed during the dark
117 cycle. As with rats used for CA2 place cell recordings, tissue samples were collected from
118 anesthetized rats immediately prior to euthanasia. Tissue samples were then stored at -20°C
119 and sent to Transnettyx Inc. to verify rats' genotypes.
120
121 *Subjects for analysis of oxytocin receptor expression.* Tissue was collected from three WT rats
122 and nine FXS rats for oxytocin receptor immunostaining. Experimenters were blinded to rat
123 genotype during tissue collection, immunostaining, imaging, and image analysis. Tissue

124 samples were collected from anesthetized rats immediately prior to terminal perfusion. Tissue
125 samples were then sent to Transnettyx Inc. for genotyping to verify rats' genotyping. Following
126 genotype verification, it was discovered that one cage had been assigned with the incorrect
127 genotype. Estimates of oxytocin receptor levels for this cage were subsequently reassigned to
128 the other genotype group. The mislabeled cage was a cage of FXS rats, which is why the FXS
129 group had more rats than the WT group.
130
131 *Subjects for in vitro recordings.* CA2 intracellular recordings were made in acute hippocampal
132 slices from four WT and four FXS male rats. Rats had free access to food and water and were
133 housed on a reverse light-dark cycle (12 hours on/ 12 hours off). Rats were 4–5 months old at
134 the time of slice preparation.
135
136 *Surgery and tetrode positioning for CA2 place cell recordings*
137 "Hyperdrive" recording devices containing 14-21 independently movable tetrodes were
138 implanted above the right dorsal hippocampus (anterior-posterior -3.8 mm from bregma, medial-
139 lateral -3.0 mm from bregma). Tetrodes were constructed from 17 µm polymide-coated
140 platinum-iridium (90/10%) wire (California Fine Wire, Grover Beach, California). The tips of the
141 tetrodes designated for single unit recording were platinum-plated to reduce single-channel
142 impedances to ~150-300 kOhms. During surgery, eleven bone screws were placed in the skull
143 and covered with dental acrylic to anchor the hyperdrive to the skull. Two of the screws were
144 connected to the recording drive ground.
145
146 On the day of surgery, all tetrodes were lowered ~1 mm into the brain. Tetrodes were then
147 slowly lowered to the hippocampal pyramidal cell body layer over several weeks except for one
148 tetrode that was designated as a reference electrode for differential recording. This tetrode was

149 placed in an electrically quiet area of cortex at least 1 mm above the hippocampal cell body
150 layer. The reference signal was duplicated using an MDR-50 breakout board (Neuralynx,
151 Bozeman, Montana) and continuously recorded to ensure that unit activity or volume conducted
152 hippocampal signals of interest (e.g., theta rhythms, sharp wave-ripples) were not detected.
153 Another tetrode was placed in the apical dendritic layer of CA1 to monitor hippocampal local
154 field potential (LFP) signals; this tetrode helped to guide placement of the other tetrodes using
155 estimated depth and electrophysiological hallmarks of the hippocampus (e.g., sharp wave-
156 ripples).
157
158 *Data acquisition for CA2 place cell experiments*
159 Data were acquired using a Digital Lynx system and Cheetah recording software (Neuralynx,
160 Bozeman, Montana). The recording setup has been described in detail previously (Zheng et al.,
161 2016). Briefly, LFP signals from one randomly chosen channel within each tetrode were
162 continuously recorded at a 2000 Hz sampling rate and filtered in the 0.1–500 Hz band. Input
163 amplitude ranges were adjusted before each recording session to maximize resolution without
164 signal saturation. Input ranges for LFPs generally fell within ±2,000 to ±3,000 μV. To detect unit
165 activity, all four channels within each tetrode were bandpass filtered from 600 to 6,000 Hz.
166 Putative spikes were detected when the filtered continuous signal on one or more of the
167 channels exceeded 55 μV. Detected events were acquired with a 32,000 Hz sampling rate for 1
168 ms. For both LFPs and unit activity, signals were recorded differentially against a dedicated
169 reference channel (see "*Surgery and tetrode positioning for CA2 place cell recordings*" section
170 above).
171
172 Videos of rats' behavior were recorded through the Neuralynx system with a resolution of 720 ×
173 480 pixels and a frame rate of 29.97 frames/s. Rat position and head direction were tracked via

174 an array of red and green or red and blue light-emitting diodes (LEDs) on a HS-54 or HS-27
175 headstage (Neuralynx, Bozeman, Montana), respectively.
176
177 *Open field behavioral task*
178 Rats were familiarized to an open field arena (1 m x 1 m with 0.5 m wall height) for a minimum
179 of three days before data collection began. Rats freely explored the open field arena for four 20-
180 minute sessions per day, with 10-minute rest sessions preceding and following each active
181 exploration session. During active exploration, small pieces of sweetened cereal or cookies
182 were randomly scattered to encourage rats to explore the entirety of the arena. Rats had to
183 cover at least 60% of the arena across each of the four sessions for a day to be included for
184 further analysis. During each rest session, rats rested in a towel-lined, elevated flowerpot
185 outside of the arena. A plexiglass standard rat housing cage was placed in one corner of the
186 arena for all recording sessions. In the first and fourth sessions (A and A'), this cage contained
187 only clean bedding. In the middle two sessions (B and B') of the different experimental
188 conditions, the cage contained social stimuli (Figure 1). In the Odor condition, a cage that had
189 formerly housed familiar rat(s) and contained soiled bedding was used. In the Visual + Odor
190 condition, a familiar rat was presented in its home cage containing soiled bedding. In the Control
191 condition, a clean cage containing only clean bedding was presented in all four sessions.
192
193 *Histology for tetrode localization for CA2 place cell recordings*
194 After place cell recordings were completed, rats were perfused with 4% paraformaldehyde
195 solution in phosphate-buffered saline. Brains were cut coronally in 30 μm sections using a
196 cryostat. For four of the rats, brain slices were stained with CA2-expressed protein striatum-
197 enriched protein-tyrosine phosphatase (STEP; Cell Signaling, 4817, 1:1000 dilution, raised in
198 mouse). Slices were then incubated in an anti-mouse secondary antibody and developed with

199 3,3-diaminobenzidine (brown) (as in Alexander et al., 2016). Slices were then counter-stained
200 with cresyl-violet (purple/blue) to indicate cell bodies. Both the presence of STEP (Figure S1A)
201 and the enlargement of cell bodies indicative of the CA2 region of the hippocampus (Lu et al.,
202 2015) (Figure S1B) were used to identify CA2. In eight of the rats, brains were immunostained
203 for CA2 marker Purkinje Cell Protein 4 (PCP4; Sigma-Aldrich Cat# HPA005792, 1:200 dilution,
204 raised in rabbit) (Figure S1C) in lieu of STEP staining. Slides were then mounted using DAPI
205 Fluoromount-G (Southern Biotech) to visualize cell bodies. Tetrode recording sites were
206 identified by comparing locations across adjacent sections.
207
208 *Spike sorting and unit selection for CA2 place cell analyses*
209 Spike sorting was performed manually using graphical cluster-cutting software (MClust, A.D.
210 Redish, University of Minnesota, Minneapolis, Minnesota) run in MATLAB (Mathworks). Spikes
211 were sorted using two-dimensional representations of waveform properties (i.e., energy, peak,
212 and peak-to-valley difference) from four channels. A single unit was accepted for further
213 analysis if the associated cluster was well isolated from, and did not share spikes with, other
214 clusters on the same tetrode. Units were also required to have a minimum 1 ms refractory
215 period. Units with mean firing rates above 5 Hz were considered putative interneurons and
216 excluded from further analysis. In order to be considered active in the arena, a unit had to reach
217 a peak firing rate of at least 1 Hz. In order to be included in the sharp wave-ripple firing analysis,
218 a unit had to have valid clusters in both the active exploration and rest sessions. CA2 cell yields
219 in each condition are reported for WT rats in Table 1 and for FXS in Table 2.
220
221 Table 1. CA2 place cell yields for WT rats.

Genotype	Rat ID	Control	Odor	Visual + Odor
WT	Rat 117 (“Lauren”)	7	5	0
WT	Rat 122 (“Chase”)	51	32	0
WT	Rat 165 (“Gus”)	34	56	26
WT	Rat 256 (“Viggo”)	28	13	13
WT	Rat 391 (“Daffodil”)	15	4	5
WT	Rat 418 (“Hugo”)	20	35	41
	Total	155	145	85

222

223 Table 2: CA2 place cell yields for FXS rats.

Genotype	Rat ID	Control	Odor	Visual + Odor
FXS	Rat 120 (“Brock”)	19	13	0
FXS	Rat 125 (“JR”)	2	3	0
FXS	Rat 330 (“Aires”)	0	1	1
FXS	Rat 395 (“Elijah”)	6	1	4
FXS	Rat 445 (“Paddy”)	7	7	5
FXS	Rat 442 (“Pippin”)	33	35	26
	Total	72	60	40

224

225 *Place cell remapping analyses*

226 Methods used to create firing rate maps for each single unit were based on established

227 methods from the place cell field that were used in our lab’s prior studies (Alexander et al.,

228 2016; Robson et al., 2025; example rate maps for the present study shown in Figure 2). First,
229 the arena was divided into 4 cm^2 bins. The number of spikes that occurred within each bin was
230 divided by the time spent in that bin to determine the firing rate. Only spikes that occurred while
231 the rat was traveling 5 cm/s or faster were included. The rate map was smoothed with a two-
232 dimensional Gaussian kernel (standard deviation = 6 cm). To determine if a place cell
233 remapped during presentation of a social stimulus, a Pearson correlation coefficient *R* was
234 calculated for each unit between pairs of rate maps from control and social stimuli sessions (i.e.,
235 A-B, B-B', B'-A', A-B', and A-A' session pairs, see Figure 1). To determine if spatial correlation
236 coefficients differed between WT and FXS rats, or across session pairs (e.g., A-B and A-A') or
237 conditions (i.e., Odor, Visual + Odor, and Control), we used a generalized linear mixed model
238 statistical analysis (IBM SPSS Statistics, version 29.0.2.0; see "*Experimental design and*
239 *statistical analysis*" section below). The estimated mean spatial correlations for each genotype
240 and condition, collapsed across session pairs, are shown in Figure 3A. Individual spatial
241 correlation values for each cell are shown for each session pair and each condition in Figure
242 3B-F.
243
244 To determine if rate remapping occurred in CA2 place cells across genotypes (i.e., WT and FXS
245 rats) and conditions (i.e., Odor, Visual + Odor, and Control), we calculated the rate overlap
246 between pairs of sessions for each place cell. The rate overlap was defined as the ratio of the
247 mean place field firing rate of the cell in each session, with the smaller of the two firing rates as
248 the numerator (as in Robson et al., 2025). This analysis allowed us to determine if CA2 place
249 cells changed their firing rates within a place field and therefore excluded cells that did not have
250 an identified place field from a given session. This allowed us to compare firing rates without the
251 confound of including cells that may gain or lose a field between sessions, which is defined as
252 global remapping, not rate remapping. To determine if rate overlap differed across genotypes

253 (i.e., WT and FXS rats), session pairs (i.e., A-B, A-B', B'-A', A-A', B-B'), and conditions (i.e.,
254 Odor, Visual + Odor, and Control), we used a generalized linear mixed model statistical analysis
255 (IBM SPSS Statistics, version 29.0.2.0; see "*Experimental design and statistical analysis*"
256 section below). The estimated mean rate overlap values for each genotype and condition,
257 collapsed across session pairs, are shown in Figure S2A. Individual rate overlap values for each
258 cell are shown for each session pair and each condition in Figure S2B-F.
259
260 *Analyses of place cell properties*
261 Spatial information (Figure 4A) was calculated as previously described (Skaggs et al., 1996)
262 using the following formula:
263 $$Spatial\ information = \sum_i P_i \frac{\lambda_i}{\lambda} log2 \frac{\lambda_i}{\lambda},$$
264 where i = the spatial bin index, P_i = the probability of the rat being in the ith bin, λ_i = the mean
265 firing rate in the ith bin, and λ = the mean firing rate of the cell.
266
267 Place fields were separately identified for each cell in each session. Potential place fields were
268 identified as contiguous bins of the smoothed rate map (see "*Place cell remapping analyses*"
269 section above) that exceeded 50% of the peak firing rate in that session. In order to be included
270 for further analysis, the peak firing rate of a place field had to exceed 1 Hz, and the size of the
271 place field had to exceed 10 cm^2.
272
273 *Exploration time analysis for open field behavioral task*
274 Exploration of the stimulus cage was quantified as previously described (Robson et al., 2025).
275 The arena was divided into 4 cm^2 bins, and the time spent in each bin during the first two
276 minutes of every session was determined for each day. These exploration maps were then

277 smoothed with a two-dimensional Gaussian kernel (standard deviation = 4 cm). Maps were
278 averaged within and then across rats within each genotype and plotted as a heat map for each
279 condition (Figure 5A-B). The time spent within 12 cm of the cage was then calculated (Figure
280 5C).
281
282 *Olfactory habituation/dishabituation task*
283 To determine if rats could detect and distinguish between social odors, we used an olfactory
284 habituation/dishabituation task (Yang & Crawley, 2009). First, rats were pre-acclimatized to the
285 test cage containing a clean dry cotton tip applicator for 15 mins to reduce novelty-induced
286 exploratory activity during the test. During the testing phase, rats were initially exposed to a
287 cotton-tip applicator with no odor for 2-3 trials ("null" trials; N1-N3 in Figure 6). This was used to
288 establish a baseline level of exploration for the object (i.e., the cotton-tip applicator). Following
289 the null trials, rats were exposed to cotton tips with an unfamiliar social odor for four consecutive
290 trials ("habituation" trials, H1-H4 in Figure 6). Following the habituation trials, rats were exposed
291 to a cotton tip with odors from a second unfamiliar social odor ("dishabituation" trial, D in Figure
292 6). All trials were 90 seconds in length. Social odors were prepared by swiping soiled home
293 cages of unfamiliar rats with cotton tip applicators. All trials were video recorded. Following
294 completion of the experiment, the time rats spent sniffing the cotton tip (within ~2 cm of the
295 cotton tip and nose pointing towards the cotton tip) during each trial was scored by two
296 independent scorers. The time spent sniffing was then averaged across the scorers. To account
297 for differences in baseline activity levels across rats, we calculated normalized difference scores
298 for each rat (*r*) and trial (*t*) using the following formula:

299 $$Norm.diff.score_{r,t} = \frac{t_r - N1_r}{t_r + N1_r}$$

300 where t_r was the sniffing time from the trial of interest for a given rat and $N1_r$ was the sniffing
301 time from the first null trial for that rat.
302
303 *Immunohistostaining for oxytocin receptors*
304 Rats (three WT rats and nine FXS rats, aged 25 weeks) were perfused in phosphate-buffered
305 saline (PBS) followed by 4% paraformaldehyde solution in PBS. Brains were stored overnight in
306 4% paraformaldehyde solution in PBS. On the day after perfusion, brains were cut coronally in
307 30 µm sections using a cryostat and mounted onto slides. Sections were kept frozen at -80
308 degrees Celsius until tissue from all rats had been collected. Immunostaining was then
309 performed simultaneously on all sections from both genotypes. First, all slides were defrosted to
310 room temperature and washed multiple times with water, boiling water, and Tris-buffered saline
311 (TBS) + 0.3% Triton X-100. Sections were then blocked for 2 hours with 5% Normal Goat
312 Serum (NGS). Sections were then incubated overnight with the following primary antibodies
313 diluted in blocking buffer: Mouse anti-RGS14 (1:1000; Antibodies Inc) and rabbit anti-oxytocin
314 receptor (1 µg/ml; Moses V. Chao, Robert C. Froemke, NYU School of Medicine Cat# OXTR-2
315 antibody, RRID:AB_2571555). The following day, slides were washed with Tris-buffered saline
316 with Tween-20 (TBST) and then incubated for two hours with the following secondary
317 antibodies: goat anti-mouse ALEXA 555, A-21422 (1:500; Thermo Fisher) and goat anti-rabbit
318 ALEXA 488, A-11008 (1:500, Thermo Fisher). Slides were then washed with TBST and TBS.
319 Lastly, slides were mounted using DAPI Fluoromount-G (Southern Biotech).
320
321 *Quantification of OXTR-2 expression*
322 Slides were imaged using a Zeiss AXIO Zoom.V16 (software Zen 3.11 Pro) microscope with an
323 Axiocam512 color camera with filters for imaging DAPI (blue, excitation range 350-360 nm,
324 emission range 460nm), Cy3 (orange-red excitation range 513-556, emission 570-613), and

325 EGFP (Enhanced Green Fluorescent Protein, excitation about 470, emission about 510) at a
326 magnification of 77x. For imaging sections that were immunostained with multiple antibodies, a
327 standardized exposure time was chosen for each filter: DAPI 200 ms, Cy3 350 ms, and EGFP
328 280 ms. The levels of oxytocin receptors in each section were estimated via the following
329 procedures. First, blinded experimenters took photomicrographs of WT and FXS sections using
330 the same microscope settings. Images were saved and subsequently analyzed by blinded
331 experimenters using Image J software (ImageJ 1.54g). Images taken with the blue (DAPI),
332 green (OXTR-2), and red (PCP4) settings were opened and calibrated to the same scale.
333 Regions of interest (i.e., CA3, CA2, and CA1) were defined in all 3 sets of images using the
334 PCP4 staining as a marker for CA2. To estimate OXTR-2 levels, background fluorescence was
335 removed, and estimates were obtained for mean fluorescence (average pixel intensity within
336 each region of interest) and total (integrated) fluorescence. To determine if OXTR-2 expression
337 differed between WT and FXS rat, or across hippocampal subregions, we used a generalized
338 linear mixed model statistical analysis (IBM SPSS Statistics, version 29.0.2.0; see
339 "*Experimental design and statistical analysis*" section below). The estimated corrected
340 fluorescence from the generalized linear mixed model for each genotype and subregion is
341 shown in Figure 7C.
342
343 *Slice preparation for in vitro recording*
344 Rats were anesthetized using a ketamine/xylazine cocktail (100/10 mg/kg) and then underwent
345 cardiac perfusions with ice-cold saline consisting of (in mM): 2.5 KCl, 1.25 NaH_2PO_4, 25
346 $NaHCO_3$, 0.5 $CaCl_2$, 7 $MgCl_2$, 7 dextrose, 205 sucrose, 1.3 ascorbic acid, and 3 sodium
347 pyruvate (bubbled constantly with 95% O_2/5% CO_2 to maintain pH at ~7.4). Following perfusion,
348 the brain was removed and sliced into 300 μM parasagittal sections from the middle
349 hippocampus using a vibrating tissue slicer (Vibratome 300, Vibratome Inc). The slices were

350 placed in a chamber filled with artificial cerebral spinal fluid (aCSF) consisting of (in mM): 125
351 NaCl, 2.5 KCl, 1.25 NaH_2PO_4, 25 $NaHCO_3$, 2 $CaCl_2$, 2 $MgCl_2$, 10 dextrose, 1.3 ascorbic acid
352 and 3 sodium pyruvate (bubbled constantly with 95% O_2/5% CO_2) for 30 minutes at 35°C and
353 then held at room temperature until time of recording.
354
355 *In vitro electrophysiology*
356 Slices were placed in a submerged, heated (33-34 C°) recording chamber and continually
357 perfused with aCSF (in mM): 125 NaCl, 3 KCl, 1.25 NaH_2PO_4, 25 $NaHCO_3$, 2 $CaCl_2$, 1 $MgCl_2$,
358 10 dextrose, and 3 sodium pyruvate (bubbled constantly with 95% O_2/5% CO_2). Ionotropic
359 glutamatergic and GABAergic synaptic transmission were blocked with 20 μM DNQX, 25 μM D-
360 AP5, and 2 μM gabazine. Pyramidal neurons within the CA2 region were visualized with a Zeiss
361 AxioScope under 60x magnification.
362
363 Current clamp recordings were made using a Dagan BVC-700 or Sutter IPA amplifier and
364 Sutterpatch acquisition software. Data were sampled at 20-50 kHz, filtered at 3 kHz, and then
365 digitized by a Dendrite interface or integrated A/D board in the Sutter IPA (Sutter). The internal
366 recording solution consisted of (in mM): 135 K-gluconate, 10 HEPES, 7 NaCl, 7 K_2-
367 phosphocreatine, 0.3 Na-GTP, 4 Mg-ATP (pH corrected to 7.3 with KOH). Recording electrodes
368 were pulled from borosilicate glass and had an open tip resistance of 4-6 MΩ. Series resistance
369 was compensated using the bridge balance circuit and was monitored throughout the
370 experiment. Recordings in which the series resistance exceeded 35 MΩ or increased by more
371 than 30% were excluded. The resting membrane potential was noted immediately after
372 establishing the whole cell recording configuration.
373
374 *Drugs for in vitro electrophysiology experiments*

375 DNQX, APV, and gabazine were purchased from Hello Bio. Thr^4-Gly^7 oxytocin (TGOT) was
376 purchased from Bachem. All drugs were prepared from a 1000x stock solution in water.
377
378 *Experimental design and statistical analyses*
379 Whenever possible, experimenters were blinded to genotype while collecting and analyzing
380 place cell data (i.e., during spike sorting). A period of limited availability of FXS rats from the
381 supplier resulted in unblinded collection and analysis of data from three rats (rats 418, 442, and
382 445). All video scoring for the olfactory habituation/dishabituation task was performed by scorers
383 blinded to genotype. Experimenters were blinded to genotype during OXTR-2 immunostaining
384 and quantification. Two experimenters conducted the in vitro electrophysiology experiments.
385 One was blinded to genotype, but the other was not.
386
387 We used a generalized linear mixed model approach (IBM SPSS version 29.0.2.0) to assess
388 differences between genotypes (i.e., WT and FXS rats) for in vivo neurophysiology, behavior,
389 and histology data. For all analyses, rats were set as the subjects, and genotype was included
390 as a fixed factor. Post-hoc tests were performed if a significant interaction or main effect was
391 observed and used the Bonferroni correction. For place cell analyses, multiple place cells were
392 nested within rats. To determine if spatial correlation coefficients (Figure 3) or rate overlap
393 values (Figure S2) differed across genotypes, conditions, and session pairs, condition and
394 session pair were included as fixed factors, and session pairs were repeated measures within
395 rats. A three-way interaction between genotype, condition, and session pair was included in the
396 model, as was a two-way interaction between genotype and condition. To assess place cell
397 properties (Figure 4), session was included as a repeated measure within rats. In addition to the
398 main effect of genotype, the model included: a three-way interaction between genotype,

399 condition, and session; a two-way interaction between genotype and session; and a two-way
400 interaction between condition and session.
401
402 To verify that our statistical tests were sufficiently powered given that a lower number of CA2
403 place cells were recorded in FXS rats than in WT rats (see Tables 1 and 2), we performed the
404 following analyses. First, we performed a simulation-based power analysis in which we
405 randomly down-sampled the number of CA2 place cells from WT rats to match the number
406 recorded in FXS rats for each condition (i.e., 72 cells in the Control condition, 60 cells in the
407 Odor condition, and 40 cells in the Visual + Odor condition) 100 times. We then used a
408 generalized linear mixed model to test for a statistically significant difference between the
409 Control condition and the Odor and Visual + Odor conditions for each simulation. We included
410 an interaction between condition and session and main effects of condition and session in the
411 model. Post-hoc comparisons were made using the Bonferroni correction when a significant
412 effect was found. We tallied the number of simulations in which the post-hoc pairwise
413 comparison showed a significant difference between the control and experimental conditions.
414 We did this separately for Control and Odor, and Control and Visual + Odor, comparisons to
415 obtain power estimates for each. We additionally ran permutation tests to compare the effects of
416 condition on spatial correlation values for each genotype and condition. The permutation tests
417 shuffled condition 1,000 times to obtain a null distribution for each spatial correlation value.
418 Monte-Carlo p-values were calculated using the formula:

$$p = \frac{N_{subset} + 1}{N_{shuffle} + 1}$$

419
420 where N_{subset} is the number of shuffles with values greater than or equal to the observed value
421 (two-tailed test), and $N_{shuffle}$ is the total number of shuffles.

422

423 To compare social stimuli exploration times across genotypes (Figure 5), days were included as
424 random factors nested within rats, as conditions were repeated on different days within rats.
425 Sessions were set as a repeated measure. In addition to the main effect of genotype, the model
426 included a three-way interaction between genotype, condition, and session and a two-way
427 interaction between condition and session.

428

429 To analyze olfactory stimuli investigation times in the habituation/dishabituation task (Figure 6),
430 trial was set as a repeated measure. In addition to the main effect of genotype, a main effect of
431 trial and a two-way interaction between genotype and trial was included in the model.

432

433 To compare the expression of oxytocin receptors across genotypes and hippocampal
434 subregions (Figure 7), multiple fluorescent estimates from brain sections were nested within
435 each subregion and set as repeated measures. In addition to genotype, subregion was included
436 as a fixed factor in the model.

437

438 Statistical tests for in vitro electrophysiology data (Figure 8) were also performed in SPSS (IBM
439 SPSS version 29.0.2.0). To compare the resting membrane potential of CA2 neurons across
440 WT and FXS rats, a univariate analysis of variance was performed with genotype as the
441 between-subjects factor. A general linear model was used to assess the effects of TGOT
442 application on CA2 neurons' resting membrane potential, with drug treatment (baseline vs.
443 TGOT) as a repeated measure and genotype as a between-subjects factor.

444

445 *Data and code availability*

446 The analysis code is available on GitHub
447 (https://github.com/mmdonahue/FMR1CA2_PUBLICSHARE). Data will be made available upon
448 reasonable request.
449
450 **Results**
451
452 *CA2 place cells in FXS rats did not remap to social stimuli*
453 Our prior studies have shown that CA2 place cells remap to social stimuli (Alexander et al.,
454 2016; Robson et al., 2025) and, specifically, that this remapping is driven by the olfactory
455 content of social stimuli (Robson et al., 2025). As FXS rats have atypical social behaviors
456 (Hamilton et al., 2014; Tian et al., 2017; Wong et al., 2020), the primary goal of this study was to
457 determine if CA2 place cells in FXS rats respond normally to the presentation of social stimuli.
458 Thus, we presented social stimuli to FXS and WT control rats while recording CA2 place cell
459 activity. We compared CA2 place cell firing patterns between WT and FXS rats across social
460 and control conditions (Figure 1).
461
462 We have previously shown that the presentation of a conspecific in a cage with soiled bedding
463 or the presentation of a soiled cage alone induces global remapping, but not rate remapping, in
464 a subset of CA2 place cells (Alexander et al., 2016; Robson et al., 2025). To test if similar
465 remapping occurs in CA2 place cells of FXS rats, we compared CA2 place cell firing patterns in
466 WT and FXS rats exploring an open field arena in which social stimuli (i.e., a familiar rat in a
467 soiled cage or a soiled cage alone) were presented. CA2 place cell firing patterns in WT and
468 FXS rats during presentation of social stimuli were compared to CA2 place cells recorded in a
469 control condition in which no social stimuli were presented in the stimulus cage (Figure 1).

470 Our recordings showed seemingly normal place cells in CA2 of FXS rats (Figure 2). To quantify
471 the extent to which CA2 place cells exhibited global remapping (i.e., a change in place cell firing
472 patterns in which place field locations change) when social stimuli were presented, we
473 calculated spatial correlation coefficients between rate maps from pairs of sessions (Figure 3).
474 We found that spatial correlation coefficients were lower for the Odor and Visual + Odor
475 conditions compared to the Control condition in WT rats (Figure 3; generalized linear mixed
476 model, no interaction between genotype, condition, and session pair ($F(20,2755) = 1.2$, $p =$
477 0.244); significant interaction between genotype and condition ($F(2,2755) = 6.9$, $p = 0.001$);
478 significant differences in post-hoc tests for WT rats for Control vs. Odor ($t(2755) = 6.5$, $p <$
479 0.001) and Control vs. Visual + Odor ($t(2755) = 6.8$, $p < 0.001$)). However, there were no
480 differences between the Control condition and either of the social conditions in FXS rats
481 (Figures 2B and 3; no differences in post-hoc tests for FXS rats for Control vs. Odor ($t(2755) =$
482 1.1, $p = 0.809$) and Control vs. Visual + Odor ($t(2755) = 0.7$, $p = 0.973$)). These results suggest
483 that CA2 place cells in FXS rats do not remap when social stimuli, namely a familiar conspecific
484 in a cage with social odors or social odors in the absence of a rat, are presented.
485
486 Because a lower number of place cells were recorded in FXS rats than in WT rats (see Tables 1
487 and 2), we performed analyses to determine whether our tests were sufficiently powered to
488 detect CA2 place cell remapping (Alexander et al., 2016; Robson et al., 2025) using the effect
489 size observed in WT rats. First, we used a simulation-based power analysis in which we the
490 number of CA2 place cells from WT rats was randomly down-sampled 100 times to match the
491 number recorded in FXS rats. We then used a generalized linear mixed model to test for a
492 statistically significant difference between the Control condition and the Odor and Visual + Odor
493 conditions for each simulation. We found that there was a significant main effect of condition
494 and a significant post-hoc pairwise comparison between the Control and Odor conditions 87%

495 of the time. There was a significant main effect of condition and a significant post-hoc pairwise
496 comparison between the Control and Visual + Odor conditions 92% of the time. We additionally
497 ran permutation tests to compare the effects of condition on spatial correlation values for each
498 genotype and condition. We found that spatial correlation values were lower in both the Odor
499 (permutation test, 1000 shuffles of condition, effect size = -0.36, $p < 0.001$) and Visual + Odor
500 (permutation test, 1000 shuffles of condition, effect size = -0.41, $p < 0.001$) conditions than in
501 the Control condition in WT rats. However, there were no significant differences between the
502 Control condition and the Odor or Visual + Odor conditions in FXS rats (Control vs. Odor:
503 permutation test, 1000 shuffles of condition, effect size = -0.09, $p = 0.27$; Control vs. Visual +
504 Odor, permutation test, 1000 shuffles of condition, effect size = -0.06, $p = 0.51$). These results
505 suggest that the lack of CA2 place cell remapping observed in FXS rats was not explained by
506 the lower number of place cells recorded in FXS rats.
507
508 Although CA2 place cells in FXS rats did not globally remap to a social stimulus, it is possible
509 that CA2 place cells respond to social stimuli by rate remapping. To test this possibility, we
510 calculated the rate overlap between pairs of sessions for CA2 place cells in WT and FXS rats
511 (Figure S2). We have previously reported that CA2 place cells did not rate remap to the
512 presentation of social stimuli in WT rats (Robson et al., 2025). In the present study, we also did
513 not observe rate remapping to social stimuli in CA2 place cells in FXS rats (generalized linear
514 mixed model, no interaction between genotype, condition, and session pair ($F(8,2718) = 0.9$, $p =$
515 0.511), no interaction between genotype and condition ($F(2,2718) = 0.8$, $p = 0.433$), no main
516 effect of genotype ($F(1,2718) < 0.1$, $p = 0.901$), no main effect of condition ($F(2,2718) = 1.4$, $p =$
517 0.252)).
518
519 *CA2 place cells exhibited normal firing properties in FXS rats*

520 The lack of remapping to social stimuli observed in CA2 place cells in FXS rats raised a
521 question of whether basic firing or spatial coding properties of CA2 place cells were abnormal in
522 FXS rats. Thus, we next assessed whether baseline firing properties of CA2 place cells differed
523 between WT and FXS rats. While CA1 place cell activity has been characterized in both FXS
524 mouse and rat models (Arbab, Battaglia, et al., 2018; Arbab, Pennartz, et al., 2018; Asiminas et
525 al., 2022; Donahue, Robson, & Colgin 2025; Talbot et al., 2018), basic firing and spatial coding
526 properties of CA2 place cells in FXS rodent models have not previously been described.
527
528 In addition to quantifying remapping across sessions in which environmental conditions change,
529 spatial correlation coefficients can also be calculated across sessions in an unchanging
530 environment to quantify place cell stability. We calculated spatial correlations between session
531 pairs in the Control condition and observed no significant differences between WT and FXS rats
532 (Figure 3; generalized linear mixed model, no difference between WT and FXS in post hoc test
533 for Control condition, $t(2755) < 0.1$, $p = 0.987$)). This suggests that the baseline stability of CA2
534 place cells in an unchanged environment is similar between WT and FXS rats.
535
536 We next examined firing properties of CA2 place cells in WT and FXS rats during individual
537 sessions. We found that spatial information transmitted by CA2 place cells did not differ
538 between WT and FXS rats across all conditions and sessions (Figure 4A; generalized linear
539 mixed model, no interaction between genotype, condition, and session ($F(8,2204) = 0.5$, $p =$
540 0.863); no interaction between genotype and session ($F(2,2204) = 0.3$, $p = 0.803$); no main
541 effect of genotype ($F(1,2204) = 0.2$, $p = 0.674$)). Average in-field firing rates (Figure 4B;
542 generalized linear mixed model, no interaction between genotype, condition, and session
543 ($F(8,2016) = 1.1$, $p = 0.366$); no interaction between genotype and session ($F(3,2016) = 1.8$, $p =$
544 0.138); no main effect of genotype ($F(1,2016) = 0.2$, $p = 0.668$)) and peak firing rates (Figure

545 4C; generalized linear mixed model, no interaction between genotype, condition, and session
546 ($F(8,2016) = 1.1$, $p = 0.340$); no interaction between genotype and session ($F(3,2016) = 1.9$, $p =$
547 0.128); no main effect of genotype ($F(1,2016) = 0.2$, $p = 0.673$)) of CA2 place cells were also
548 similar between WT and FXS rats. Also, CA2 place field size (Figure 4D; generalized linear
549 mixed model, no interaction between genotype, condition, and session ($F(8,2016) = 0.2$, $p =$
550 0.277); no interaction between genotype and session ($F(3,2016) = 0.3$, $p = 0.857$); no main
551 effect of genotype ($F(1,2016) = 0.8$, $p = 0.380$)) and average number of place fields per place
552 cell per session (Figure 4E; generalized linear mixed model, no interaction between genotype,
553 condition, and session ($F(8,2204) = 0.9$, $p = 0.539$); no interaction between genotype and
554 session ($F(3,2204) = 1.3$, $p = 0.263$); no main effect of genotype ($F(1,2204) = 0.7$, $p = 0.389$))
555 did not differ between WT and FXS rats. Altogether, these results indicate that CA2 place cells
556 represent spatial locations similarly in FXS and WT rats.
557
558 *FXS rats explored and perceived social stimuli normally*
559 A possible explanation of why CA2 place cells failed to remap to social stimuli in FXS rats could
560 be reduced exploration of, or attention to, social stimuli in FXS rats. To explore this possibility,
561 we calculated the amount of time spent exploring the stimulus cage across conditions for WT
562 rats and FXS rats (Figure 5). We first created heat maps to visualize the amount of time rats
563 spent exploring locations across the open field arena and noted that both WT and FXS rats
564 spent a high amount of time near the stimulus cage in the Odor and Visual + Odor conditions
565 (Figure 5A-B). To quantify these observations, we calculated the time spent near the stimulus
566 cage across conditions and sessions for all rats. We found that both WT and FXS groups of rats
567 increased the time they spent near the stimulus cage in Session B during the Odor and Visual +
568 Odor conditions (Figure 5C; generalized linear mixed model, no interaction between genotype,
569 condition, and session ($F(11,260) = 0.4$, $p = 0.935$); significant interaction between condition

570 and session ($F(11,260) = 5.4$, $p < 0.001$); significant differences in post-hoc tests for Session B
571 for Control vs. Odor ($t(260) = -5.3$, $p < 0.001$) and Control vs. Visual + Odor ($t(260) = -4.1$, $p <$
572 0.001)). This indicates that WT and FXS rats explored social stimuli to a similar extent.
573
574 We have previously shown that the olfactory content of social stimuli is necessary for CA2 place
575 cell remapping to social stimuli (Robson et al., 2025). Although structural and functional
576 changes have been identified in the olfactory system of FXS rodent models (Bodaleo et al.,
577 2019), these differences appear to impact olfactory sensitivity and fine odor discrimination, but
578 not the detection of odors or the discrimination of monomolecular odors (Kuruppath et al., 2023;
579 Nitenson et al., 2015). Still, it is possible that impaired olfactory perception of social stimuli
580 explains the lack of CA2 place cell remapping to social stimuli in FXS rats. To assess whether
581 olfactory perception and discrimination were impaired in FXS rats, we assessed olfactory
582 function in FXS rats using an olfactory habituation/dishabituation task (Figure 6). This task tests
583 rats' ability to recognize an odor when it is initially presented, habituate to the presence of the
584 same odor across repeated presentations ("habituation" trials), and distinguish between odors
585 after the presentation of a novel odor in the last trial ("dishabituation" trial). We found that FXS
586 rats could detect the presence of a social odor normally during the first habituation trial (Figure
587 6; generalized linear mixed model, no interaction between genotype and trial ($F(7,259) = 0.6$, p
588 $= 0.722$); significant main effect of trial ($F(1,259) = 126.9$, $p < 0.001$); significant differences in
589 post-hoc tests for Null 1 vs. Habituation 1 ($t(259) = -4.2$, $p = 0.001$), Null 2 vs. Habituation 1
590 ($t(259) = -7.4$, $p < 0.001$), Null 3 vs. Habituation 1 ($t(259) = -9.8$, $p < 0.001$)). Further, both WT
591 and FXS rats decreased their sniffing of the same social odor across repeated presentations
592 (significant difference in post-hoc test for Habituation 1 vs. Habituation 4 ($t(259) = 9.2$, $p <$
593 0.001)), indicating normal habituation to a social odor in FXS rats. FXS rats also increased their
594 sniffing in the same manner as WT rats when a novel social odor was introduced during the

595 dishabituation trial (significant difference in post-hoc test for Habituation 4 vs. Dishabituation
596 ($t(259) = -8.7$, $p < 0.001$)). This indicates that FXS rats detected social odors, and distinguished
597 between different social odors, in the same way as WT rats.
598
599 *Impaired oxytocin modulation of area CA2 in FXS rats*
600 The neuropeptide oxytocin plays a key role in social behaviors and social memory (Froemke &
601 Young 2022). High expression of oxytocin receptors is a characteristic feature of area CA2
602 (Mitre et al. 2016), and oxytocin receptors in CA2 are essential for social functions (Raam et al.
603 2017, Lin et al. 2018, Tsai et al. 2022). Thus, we hypothesized that reduced responses to social
604 stimuli in CA2 place cells could be due to deficient oxytocin receptor expression in CA2 of FXS
605 rats. To test this hypothesis, we immunostained hippocampal tissue from WT and FXS rats with
606 OXTR-2, an antibody that is highly specific for oxytocin receptors (Mitre et al. 2016). We then
607 compared expression of oxytocin receptors in area CA2, and neighboring subregions CA1 and
608 CA3, in WT and FXS rats (Figure 7). Significant differences in the mean intensity of OXTR-2
609 immunostaining were observed across subregions and genotypes (Figure 7C; generalized linear
610 mixed model, significant interaction between genotype and subregion ($F(2,701) = 17.1$, $p <$
611 0.001)). In WT rats, oxytocin receptor expression levels were higher in CA2 than in CA1 and
612 CA3 (generalized linear mixed model, significant main effect of subregion for WT rats ($F(2,174)$
613 $= 93.7$, $p < 0.001$) and significant differences in post-hoc tests for CA1 vs. CA2 ($p < 0.001$) and
614 CA3 vs CA2 ($p < 0.001$)), as expected based on earlier results from WT mice (Mitre et al. 2016).
615 Similarly, oxytocin receptor expression in FXS rats was higher in CA2 than in CA1 and CA3
616 (generalized linear mixed model, significant main effect of subregion for FXS rats ($F(2,527) =$
617 459.7, $p < 0.001$) and significant differences in pairwise comparisons for CA1 vs. CA2 ($p <$
618 0.001) and CA3 vs CA2 ($p < 0.001$)). We additionally found that oxytocin receptor expression
619 levels were significantly lower in FXS rats than in WT rats across all subregions (generalized

620 linear mixed model, significant main effect of genotype ($F(1,701) = 160.9$, $p < 0.001$)) and in
621 CA2 tested individually (generalized linear mixed model, significant main effect of genotype
622 ($F(1,233) = 9.8$, $p = 0.002$)). These results raise the possibility that reduced responses to
623 oxytocin in CA2 neurons contribute to diminished responses to social stimuli observed in CA2
624 place cells in FXS rats.
625
626 Thus, we next tested whether CA2 neurons in FXS rats exhibit reduced responses to oxytocin
627 receptor activation. Prior work in WT mice showed that CA2 neurons depolarize in response to
628 oxytocin, and such depolarizing responses were proposed to promote social remapping in CA2
629 (Tirko et al. 2018). Accordingly, we hypothesized that CA2 neurons would depolarize in
630 response to oxytocin administration in slices from WT rats but not FXS rats. To test this
631 hypothesis, we performed whole-cell current clamp recordings of CA2 pyramidal neurons and
632 tested how bath application of the specific oxytocin receptor agonist Thy^4,Gly^7-oxytocin (TGOT,
633 400 nM) affected the resting membrane potential. First, we found that the baseline resting
634 membrane potential of CA2 pyramidal neurons was more hyperpolarized in FXS slices than in
635 WT slices (Figure 8; $n = 6$ cells from 4 rats of each genotype, univariate analysis of variance,
636 genotype as between-subjects factor, significant effect of genotype ($F(1,10) = 5.0$, $p = 0.05$)).
637 Next, we found that TGOT administration affected FXS and WT neurons differently (Figure 8;
638 general linear model with genotype as between-subjects-factor and drug treatment as repeated
639 measure within subjects, significant interaction between genotype and drug treatment ($F(1,10) =$
640 5.4, $p = 0.04$)). Specifically, TGOT application significantly depolarized CA2 pyramidal cells in
641 slices from WT rats (significant difference in post-hoc pairwise comparison for WT rats for
642 baseline vs. TGOT (ΔV_M: 3.8 ± 0.83 mV; $t(5) = -4.6$, $p = 0.006$)), as expected (Tirko et al. 2018).
643 In contrast, CA2 pyramidal neurons in slices from FXS rats did not significantly depolarize in

644 response to TGOT application (no significant difference for FXS rats for baseline vs. TGOT
645 (ΔV_M: 1.2 ± 0.79 mV; $t(5) = -1.472$, $p = 0.201$)). These results suggest that deficient responses
646 to oxytocin in CA2 neurons may hinder activation of CA2 neurons by social stimuli and thereby
647 contribute to deficits in social remapping observed in CA2 place cells in FXS rats.
648
649 **Discussion**
650 A large number of studies have identified abnormalities in social behaviors in mouse and rat
651 models of FXS (Hamilton et al., 2014; Liu & Smith, 2009; McNaughton et al., 2008; Mineur et
652 al., 2006; Oddi et al., 2014; Saxena et al., 2018; Spencer et al., 2005; Tian et al., 2017; Wong et
653 al., 2020). In this study, we identified a neurophysiological difference in responses to social
654 stimuli in CA2 place cells of FXS rats. We have previously shown that a significant proportion of
655 CA2 place cells in WT rats changed their firing fields when a familiar rat in a soiled cage was
656 presented (Alexander et al., 2016; Robson et al., 2025) or when a soiled home-cage was
657 presented without a rat (Robson et al., 2025). In contrast, the present study revealed that CA2
658 place cells in FXS rats did not change their firing fields when social stimuli were presented. This
659 lack of social remapping in CA2 of FXS rats was not explained by reduced exploration of social
660 stimuli or a lack of olfactory discrimination in FXS rats. Furthermore, we found no differences in
661 firing rates, spatial information coding, and basic place field properties in CA2 place cells in FXS
662 rats, suggesting that impairments in CA2 place cell activity in FXS rats were largely specific to
663 responses to social stimuli.
664
665 To our knowledge, this study is the first to record CA2 place cells in a rodent model of FXS. We
666 found no abnormalities in baseline firing rates or spatial coding in CA2 neurons in FXS rats.
667 However, our experiments exclusively involved familiar environments and stimuli. Environmental
668 novelty has been shown to differentially affect CA1 place cells in FXS rats (Asiminas et al.,

669 2022). Specifically, CA1 place cells in FXS rats do not undergo normal experience-dependent
670 changes in spatial selectivity or firing rates (Asiminas et al., 2022). Therefore, it is possible that
671 CA2 place cell properties would differ between WT and FXS rats across experience in a novel
672 environment. Future experiments examining CA2 place cell firing patterns in FXS rats exploring
673 novel environments will be important to determine if CA2 place cell firing properties are
674 differentially affected by experience in WT and FXS rats.
675
676 Multiple studies have shown that CA2 place cells alter their firing fields during social interactions
677 (Alexander et al., 2016; Oliva et al., 2020; Robson et al., 2025), but the mechanism underlying
678 this social remapping has not yet been identified. Therefore, it is possible that impairments in
679 CA2 place cell remapping in FXS rats may be inherited from upstream regions or may be due to
680 impaired local computations within CA2. CA2 is unique as a hippocampal subregion in that it
681 contains an abundance of neuropeptide receptors, including oxytocin. In mice, blocking or
682 ablating oxytocin receptors in CA2 impairs social memory (Lin et al., 2018; Raam et al., 2017;
683 Tsai et al., 2022), and CA2 neurons are depolarized by activation of oxytocin receptors (Tirko et
684 al., 2018). It is therefore possible that the release of oxytocin in CA2 during social interactions
685 promotes changes in CA2 place cell firing patterns. If so, a dysregulation of oxytocin release,
686 reduced expression of oxytocin receptors, or impaired oxytocin signaling in CA2 of FXS rats
687 could contribute to the lack of remapping to social stimuli observed in FXS rats in this study. In
688 FXS rats in the present study, we identified reductions in oxytocin receptor expression levels
689 and impaired depolarizing responses to oxytocin in CA2 neurons. These oxytocinergic
690 impairments may contribute to deficient place cell coding of social stimuli in the following
691 manner. Depolarizing oxytocinergic inputs to CA2 may offset strong inhibitory inputs to CA2
692 neurons (Chevaleyre and Siegelbaum, 2010), thereby allowing some CA2 neurons to develop a
693 new place field in response to social stimuli. Considering that the overall level of activity in the

694 place cell network is thought to be homeostatically maintained (Kaleb et al., 2021), newly
695 activated place cells could trigger network competition and local inhibition within CA2, causing
696 some previously active cells to lose their place fields. In this way, activation of oxytocin
697 receptors on CA2 place cells could promote remapping to social stimuli in WT rats. In contrast,
698 diminished oxytocin receptor expression and weakened depolarizing responses to oxytocin
699 could hinder CA2 place cell remapping to social stimuli in FXS rats.
700
701 Oxytocin release in CA2 has not yet been characterized in FXS models, but reduced oxytocin
702 release may also potentially contribute to these deficits. Oxytocin receptors are overexpressed
703 in several subregions of the hippocampus, including CA2, in a separate rodent model of autism,
704 potentially as a compensatory mechanism for reduced oxytocin release (Bertoni et al., 2021).
705 Previous work has also shown that the oxytocin-mediated excitatory/inhibitory shift of GABA is
706 impaired in a mouse model of FXS (Tyzio et al., 2014), and that treatments that rescue this
707 impairment prenatally result in improvements in social behavior in adulthood (Eftekhari et al.,
708 2014). Related to this, an important question to be examined in future studies is whether
709 oxytocin administration (e.g., oxytocin uncaging; Ahmed et al., 2023) can rescue CA2 place cell
710 remapping in FXS rats.
711
712 CA2 receives direct inputs from other brain regions involved in social processing that may be
713 important for transmitting social information to CA2 and driving social responses in place cells.
714 The direct projection from the lateral entorhinal cortex to CA2 is necessary for social memory
715 (Dang et al., 2022; Lopez-Rojas et al., 2022). This direct projection arises from layer II
716 entorhinal cortical neurons (Dang et al., 2022). To our knowledge, layer II entorhinal cortical
717 neurons have not been examined in a rodent model of FXS, but neurons in other layers of the
718 entorhinal cortex show abnormal physiological properties in FXS mice (Deng et al., 2013; Deng

719 & Klyachko, 2016). Thus, an interesting hypothesis to test in future studies is the extent to which
720 abnormal physiology in the direct projection from the lateral entorhinal cortex to CA2 contributes
721 to impaired CA2 place cell remapping to social stimuli in FXS rats.
722
723 The function of CA2 place cell remapping to social stimuli remains unclear. Dorsal CA2, the
724 area from which the place cells in this study were recorded, projects directly to ventral CA1
725 (Meira et al., 2018; Okuyama et al., 2016), and this pathway is essential for social memory
726 (Meira et al., 2018; Tsai et al., 2022). Exogenous activation of this pathway rescues social
727 memory deficits in a mouse model of autism (Cope et al., 2023) and in an oxytocin receptor
728 knockout mouse (Tsai et al., 2022). Also, the direct projection from ventral CA1 to the prefrontal
729 cortex is important for social memory (Phillips et al., 2019; Sun et al., 2020). Hyperexcitability in
730 this pathway has been shown to contribute to social memory impairments in a mouse model of
731 autism (Phillips et al., 2019). While this pathway has not been specifically examined in FXS
732 models, FXS mice show reduced coherence between the ventral hippocampus and the
733 prefrontal cortex (Bhandari et al., 2024), providing a potential mechanistic link between impaired
734 CA2 place cell remapping in FXS rats and abnormal social behaviors.
735
736 However, the possibility remains that CA2 place cell remapping to social stimuli is
737 epiphenomenal. CA2 place cells also remap to the presentation of novel objects (Alexander et
738 al., 2016; Oliva et al., 2020), but optogenetic silencing of CA2 neurons does not impact
739 performance on a novel object recognition task (Oliva et al., 2020). Although inactivation of CA2
740 impairs social memory (Hitti & Siegelbaum, 2014; Leroy et al., 2017; Oliva et al., 2020;
741 Stevenson & Caldwell, 2014), it is difficult to establish if the change of firing fields in response to
742 social conditions is necessary for social memory or if a more general CA2 signal is sufficient. It
743 is possible that the impaired CA2 remapping to social stimuli in FXS rats may not functionally

744 contribute to abnormal social behaviors. Future studies are necessary to establish whether CA2
745 place cell remapping has functional consequences for social behaviors and, if so, how
746 impairments in CA2 place cell remapping may contribute to abnormal social behaviors in FXS
747 rats. Establishing these connections may help provide novel treatment targets that specifically
748 address social behavioral impairments in patients with FXS.
749

750 **References**

751 Ahmed, I. A., Liu, J.-J., Gieniec, K. A., Bair-Marshall, C. J., Adewakun, A. B., Hetzler, B. E., Arp,
752 C. J., Khatri, L., Vanwalleghem, G. C., Seidenberg, A. T., Cowin, P., Trauner, D., Chao,
753 M. V., Davis, F. M., Tsien, R. W., & Froemke, R. C. (2023). Optopharmacological tools for
754 precise spatiotemporal control of oxytocin signaling in the central nervous system and
755 periphery. *Research Square*, rs.3.rs-2715993. https://doi.org/10.21203/RS.3.RS-
756 2715993/V1

757 Alexander, G. M., Farris, S., Pirone, J. R., Zheng, C., Colgin, L. L., & Dudek, S. M. (2016). Social
758 and novel contexts modify hippocampal CA2 representations of space. *Nature*
759 *Communications*, *7*(1), 1–14. https://doi.org/10.1038/ncomms10300

760 Arbab, T., Battaglia, F. P., Pennartz, C. M. A., & Bosman, C. A. (2018). Abnormal hippocampal
761 theta and gamma hypersynchrony produces network and spike timing disturbances in the
762 Fmr1-KO mouse model of Fragile X syndrome. *Neurobiology of Disease*, *114*(1), 65–73.
763 https://doi.org/10.1016/j.nbd.2018.02.011

764 Arbab, T., Pennartz, C. M. A., & Battaglia, F. P. (2018). Impaired hippocampal representation of
765 place in the Fmr1-knockout mouse model of fragile X syndrome. *Scientific Reports*, 8(1),
766 1–9. https://doi.org/10.1038/s41598-018-26853-z

767 Ashley, C. T., Wilkinson, K. D., Reines, D., & Warren, S. T. (1993). FMR1 protein: conserved RNP
768 family domains and selective RNA binding. *Science*, 262(5133), 563–566.
769 https://doi.org/10.1126/SCIENCE.7692601

770 Asiminas, A., Booker, S. A., Dando, O. R., Kozic, Z., Arkell, D., Inkpen, F. H., Sumera, A., Akyel,
771 I., Kind, P. C., & Wood, E. R. (2022). Experience-dependent changes in hippocampal
772 spatial activity and hippocampal circuit function are disrupted in a rat model of Fragile X
773 Syndrome. *Molecular Autism*, 13(1), 1–29. https://doi.org/10.1186/s13229-022-00528-z

774 Bakker, C. E., Verheij, C., Willemsen, R., van der Helm, R., Oerlemans, F., Vermey, M., Bygrave,
775 A., Hoogeveen, A. T., Oostra, B. A., Reyniers, E., De Boule, K., D'Hooge, R., Cras, P.,
776 van Velzen, D., Nagels, G., Martin, J. J., De Deyn, P. P., Darby, J. K., & Willems, P. J.
777 (1994). Fmr1 knockout mice: A model to study fragile X mental retardation. *Cell*, 78(1),
778 23–33. https://doi.org/10.1016/0092-8674(94)90569-X

779 Bertoni, A., Schaller, F., Tyzio, R., Gaillard, S., Santini, F., Xolin, M., Diabira, D., Vaidyanathan,
780 R., Matarazzo, V., Medina, I., Hammock, E., Zhang, J., Chini, B., Gaiarsa, J. L., &
781 Muscatelli, F. (2021). Oxytocin administration in neonates shapes hippocampal circuitry

and restores social behavior in a mouse model of autism. *Molecular Psychiatry*, 26(12), 7582–7595. https://doi.org/10.1038/s41380-021-01227-6

Bhandari, K., Kanodia, H., Donato, F., & Caroni, P. (2024). Selective vulnerability of the ventral hippocampus-prelimbic cortex axis parvalbumin interneuron network underlies learning deficits of fragile X mice. *Cell Reports*, 43(5), 114124. https://doi.org/10.1016/j.celrep.2024.114124

Bodaleo, F., Tapia-Monsalves, C., Cea-Del Rio, C., Gonzalez-Billault, C., & Nunez-Parra, A. (2019). Structural and functional abnormalities in the olfactory system of fragile x syndrome models. *Frontiers in Molecular Neuroscience*, 12, 448197. https://doi.org/10.3389/FNMOL.2019.00135/BIBTEX

Chevaleyre, V., & Siegelbaum, S. A. (2010). Strong CA2 pyramidal neuron synapses define a powerful disynaptic cortico-hippocampal loop. Neuron, 66(4), 560-572.

Colgin, L. L., Moser, E. I., & Moser, M. B. (2008). Understanding memory through hippocampal remapping. *Trends in Neurosciences*, 31(9), 469–477. https://doi.org/10.1016/j.tins.2008.06.008

Cope, E. C., Wang, S. H., Waters, R. C., Gore, I. R., Vasquez, B., Laham, B. J., & Gould, E. (2023). Activation of the CA2-ventral CA1 pathway reverses social discrimination dysfunction in Shank3B knockout mice. *Nature Communications*, 14(1), 1–16. https://doi.org/10.1038/s41467-023-37248-8

Dang, R., Zhou, Y., Zhang, Y., Liu, D., Wu, M., Liu, A., Jia, Z., Xie, W. (2022). Regulation of social memory by lateral entorhinal cortical projection to dorsal hippocampal CA2. *Neuroscience Bulletin*, 38(3), 318–322. https://doi.org/10.1007/s12264-021-00813-6

Deng, P. Y., & Klyachko, V. A. (2016). Increased persistent sodium current causes neuronal hyperexcitability in the entorhinal cortex of Fmr1 knockout mice. *Cell Reports*, 16(12), 3157–3166. https://doi.org/10.1016/j.celrep.2016.08.046

Deng, P. Y., Rotman, Z., Blundon, J. A., Cho, Y., Cui, J., Cavalli, V., Zakharenko, S. S., & Klyachko, V. A. (2013). FMRP regulates neurotransmitter release and synaptic information transmission by modulating action potential duration via BK channels. *Neuron*, 77(4), 696–711. https://doi.org/10.1016/j.neuron.2012.12.018

Donahue, M. M., Robson, E., & Colgin, L. L. (2025). Hippocampal place cell sequences are impaired in a rat model of Fragile X Syndrome. *Journal of Neuroscience*, 45(15).

Eftekhari, S., Shahrokhi, A., Tsintsadze, V., Nardou, R., Brouchoud, C., Conesa, M., Burnashev, N., Ferrari, D. C., & Ben-Ari, Y. (2014). Response to comment on “Oxytocin-mediated GABA inhibition during delivery attenuates autism pathogenesis in rodent offspring.” *Science*, 346(6206). https://doi.org/10.1126/SCIENCE.1256009/ASSET/42325DA6-71A9-4A0B-8740-0AB20FCDBC61/ASSETS/GRAPHIC/346_176C_F1.JPEG

Froemke, R. C., & Young, L. J. (2021). Oxytocin, neural plasticity, and social behavior. *Annual Review of Neuroscience*, 44(1), 359-381.

Hamilton, S. M., Green, J. R., Veeraragavan, S., Yuva, L., McCoy, A., Wu, Y., Warren, J., Little, L., Ji, D., Cui, X., Weinstein, E., & Paylor, R. (2014). Fmr1 and Nlgn3 knockout rats: Novel tools for investigating autism spectrum disorders. *Behavioral Neuroscience*, 128(2), 103–109. https://doi.org/10.1037/a0035988

Hitti, F. L., & Siegelbaum, S. A. (2014). The hippocampal CA2 region is essential for social memory. *Nature*, 508(1), 88–92. https://doi.org/10.1038/nature13028

Jin, P., & Warren, S. T. (2000). Understanding the molecular basis of fragile X syndrome. *Human Molecular Genetics*, 9(6), 901–908. https://doi.org/10.1093/HMG/9.6.901

Kaleb, K., Pedrosa, V., & Clopath, C. (2021). Network-centered homeostasis through inhibition maintains hippocampal spatial map and cortical circuit function. Cell Reports, 36(8).

Kau, A. S. M., Tierney, E., Bukelis, I., Stump, M. H., Kates, W. R., Trescher, W. H., & Kaufmann, W. E. (2004). Social behavior profile in young males with fragile X syndrome: Characteristics and specificity. *American Journal of Medical Genetics*, 126A(1), 9–17. https://doi.org/10.1002/AJMG.A.20218

Kaufmann, W. E., Cortell, R., Kau, A. S. M., Bukelis, I., Tierney, E., Gray, R. M., Cox, C., Capone, G. T., & Stanard, P. (2004). Autism spectrum disorder in fragile X syndrome: Communication, social interaction, and specific behaviors. *American Journal of Medical Genetics*, 129A(3), 225–234. https://doi.org/10.1002/AJMG.A.30229

Kuruppath, P., Xue, L., Pouille, F., Jones, S. T., & Schoppa, N. E. (2023). Hyperexcitability in the olfactory bulb and impaired fine odor discrimination in the Fmr1 KO mouse model of Fragile X Syndrome. *Journal of Neuroscience*, 43(48), 8243–8258. https://doi.org/10.1523/JNEUROSCI.0584-23.2023

Leroy, F., Brann, D. H., Meira, T., & Siegelbaum, S. A. (2017). Input-timing-dependent plasticity in the hippocampal CA2 region and its potential role in social memory. *Neuron*, 95(5), 1089-1102.e5. https://doi.org/10.1016/j.neuron.2017.07.036

Lesniak-Karpiak, K., Mazzocco, M. M. M., & Ross, J. L. (2003). Behavioral assessment of social anxiety in females with Turner or Fragile X Syndrome. *Journal of Autism and Developmental Disorders*, 33(1), 55–67. https://doi.org/10.1023/A:1022230504787/METRICS

Lin, Y. T., Hsieh, T. Y., Tsai, T. C., Chen, C. C., Huang, C. C., & Hsu, K. Sen. (2018). Conditional deletion of hippocampal CA2/CA3a oxytocin receptors impairs the persistence of long-term social recognition memory in mice. *Journal of Neuroscience*, 38(5), 1218–1231. https://doi.org/10.1523/JNEUROSCI.1896-17.2017

Liu, Z. H., & Smith, C. B. (2009). Dissociation of social and nonsocial anxiety in a mouse model of fragile X syndrome. *Neuroscience Letters*, 454(1), 62–66. https://doi.org/10.1016/J.NEULET.2009.02.066

Lopez-Rojas, J., de Solis, C. A., Leroy, F., Kandel, E. R., & Siegelbaum, S. A. (2022). A direct lateral entorhinal cortex to hippocampal CA2 circuit conveys social information required for social memory. *Neuron*, 110(9), 1559-1572.e4. https://doi.org/10.1016/j.neuron.2022.01.028

Lu, L., Igarashi, K. M., Witter, M. P., Moser, E. I., & Moser, M. B. (2015). Topography of place maps along the CA3-to-CA2 axis of the hippocampus. *Neuron*, 87(5), 1078-1092. https://doi.org/10.1016/j.neuron.2015.07.007

McNaughton, C. H., Moon, J., Strawderman, M. S., Maclean, K. N., Evans, J., & Strupp, B. J. (2008). Evidence for social anxiety and impaired social cognition in a mouse model of Fragile X Syndrome. *Behavioral Neuroscience*, 122(2), 293–300. https://doi.org/10.1037/0735-7044.122.2.293

Meira, T., Leroy, F., Buss, E. W., Oliva, A., Park, J., & Siegelbaum, S. A. (2018). A hippocampal circuit linking dorsal CA2 to ventral CA1 critical for social memory dynamics. *Nature Communications*, 9(1), 1–14. https://doi.org/10.1038/s41467-018-06501-w

Merenstein, S. A., Sobesky, W. E., Taylor, A. K., Riddle, J. E., Ran, H. X. ", & Hagerman, R. J. (1996). Molecular-clinical correlations in males with an expanded FMR1 mutation. *American Journal of Medical Genetics*, 64, 388–394. https://doi.org/10.1002/(SICI)1096-8628(19960809)64:2

Mientjes, E. J., Nieuwenhuizen, I., Kirkpatrick, L., Zu, T., Hoogeveen-Westerveld, M., Severijnen, L., Rifé, M., Willemsen, R., Nelson, D. L., & Oostra, B. A. (2006). The generation of a conditional Fmr1 knock out mouse model to study Fmrp function in vivo. *Neurobiology of Disease*, 21(3), 549–555. https://doi.org/10.1016/J.NBD.2005.08.019

Mineur, Y. S., Huynh, L. X., & Crusio, W. E. (2006). Social behavior deficits in the Fmr1 mutant mouse. *Behavioural Brain Research*, 168(1), 172–175. https://doi.org/10.1016/J.BBR.2005.11.004

Mitre, M., Marlin, B. J., Schiavo, J. K., Morina, E., Norden, S. E., Hackett, T. A., Aoki, C. J., Chao, M. V., Froemke, R. C. (2016). A distributed network for social cognition enriched for oxytocin receptors. *Journal of Neuroscience*, 36(8), 2517–2535. https://doi.org/10.1523/jneurosci.2409-15.2016

Nitenson, A. S., Stackpole, E. E., Truszkowski, T. L. S., Midroit, M., Fallon, J. R., & Bath, K. G. (2015). Fragile X Mental Retardation Protein regulates olfactory sensitivity but not odorant discrimination. *Chemical Senses*, 40(5), 345–350. https://doi.org/10.1093/CHEMSE/BJV019

O'Keefe, J., & Dostrovsky, J. (1971). The hippocampus as a spatial map. Preliminary evidence from unit activity in the freely-moving rat. *Brain Research*, 34(1), 171–175. https://doi.org/10.1016/0006-8993(71)90358-1

Oddi, D., Subashi, E., Middei, S., Bellocchio, L., Lemaire-Mayo, V., Guzmán, M., Crusio, W. E., D'Amato, F. R., & Pietropaolo, S. (2014). Early social enrichment rescues adult behavioral and brain abnormalities in a mouse model of Fragile X Syndrome. *Neuropsychopharmacology*, 40(5), 1113–1122. https://doi.org/10.1038/npp.2014.291

Okuyama, T., Kitamura, T., Roy, D. S., Itohara, S., Tonegawa, S. (2016). Ventral CA1 neurons store social memory. *Science*. https://doi.org/10.1126/science.aaf7003

Oliva, A. (2022). CA2 physiology underlying social memory. *Current Opinion in Neurobiology*, 77, 102642. https://doi.org/10.1016/j.conb.2022.102642

Oliva, A., Fernández-Ruiz, A., Leroy, F., & Siegelbaum, S. A. (2020). Hippocampal CA2 sharp-wave ripples reactivate and promote social memory. *Nature*, 587(7833), 264–269. https://doi.org/10.1038/s41586-020-2758-y

Pagani, J. H., Zhao, M., Cui, Z., Avram, S. K. W., Caruana, D. A., Dudek, S. M., Young, W. S. (2015). Role of the vasopressin 1b receptor in rodent aggressive behavior and synaptic plasticity in hippocampal area CA2. *Molecular Psychiatry*, 20(4), 490–499. https://doi.org/10.1038/mp.2014.47

Phillips, M. L., Robinson, H. A., & Pozzo-Miller, L. (2019). Ventral hippocampal projections to the medial prefrontal cortex regulate social memory. *eLife*, 8. https://doi.org/10.7554/ELIFE.44182

Pieretti, M., Zhang, F., Fu, Y. H., Warren, S. T., Oostra, B. A., Caskey, C. T., & Nelson, D. L. (1991). Absence of expression of the FMR-1 gene in fragile X syndrome. *Cell*, 66(4), 817–822. https://doi.org/10.1016/0092-8674(91)90125-I

Raam, T., McAvoy, K. M., Besnard, A., Veenema, A. H., Sahay, A. (2017). Hippocampal oxytocin receptors are necessary for discrimination of social stimuli. *Nature Communications*, 8(1), 2001. https://doi.org/10.1038/s41467-017-02173-0

Richter, J. D., & Zhao, X. (2021). The molecular biology of FMRP: new insights into fragile X syndrome. *Nature Reviews Neuroscience*, 22(4), 209–222. https://doi.org/10.1038/s41583-021-00432-0

Robson, E., Donahue, M. M., Mably, A. J., Demetrovich, P. G., Hewitt, L. T., & Colgin, L. L. (2025). Social odors drive hippocampal CA2 place cell responses to social stimuli. *Progress in neurobiology*, 245, 102708.

Saxena, K., Webster, J., Hallas-Potts, A., Mackenzie, R., Spooner, P. A., Thomson, D., Kind, P., Chatterji, S., & Morris, R. G. M. (2018). Experiential contributions to social dominance in a rat model of fragile-X syndrome. *Proceedings of the Royal Society B: Biological Sciences*, 285(1880). https://doi.org/10.1098/RSPB.2018.0294

Siomi, H., Siomi, M. C., Nussbaum, R. L., & Dreyfuss, G. (1993). The protein product of the fragile X gene, FMR1, has characteristics of an RNA-binding protein. *Cell*, 74(2), 291–298. https://doi.org/10.1016/0092-8674(93)90420-U

Skaggs, W. E., McNaughton, B. L., Wilson, M. A., & Barnes, C. A. (1996). Theta phase precession in hippocampal neuronal populations and the compression of temporal sequences. *Hippocampus*, 6(2), 149–172. https://doi.org/10.1002/(sici)1098-1063(1996)6:2<149::aid-hipo6>3.0.co;2-K

Spencer, C. M., Alekseyenko, O., Serysheva, E., Yuva-Paylor, L. A., & Paylor, R. (2005). Altered anxiety-related and social behaviors in the Fmr1 knockout mouse model of fragile X syndrome. *Genes, Brain and Behavior*, 4(7), 420–430. https://doi.org/10.1111/J.1601-183X.2005.00123.X

Stevenson, E. L., & Caldwell, H. K. (2014). Lesions to the CA2 region of the hippocampus impair social memory in mice. *European Journal of Neuroscience*, 40(9), 3294–3301. https://doi.org/10.1111/ejn.12689

Sun, Q., Li, X., Li, A., Zhang, J., Ding, Z., Gong, H., & Luo, Q. (2020). Ventral hippocampal-prefrontal interaction affects social behavior via parvalbumin positive neurons in the medial prefrontal cortex. *iScience*, 23(3), 100894. https://doi.org/10.1016/j.isci.2020.100894

Talbot, Z. N., Sparks, F. T., Dvorak, D., Curran, B. M., Alarcon, J. M., & Fenton, A. A. (2018). Normal CA1 place fields but discoordinated network discharge in a Fmr1-null mouse model of Fragile X Syndrome. *Neuron*, 97(3), 684-697.e4. https://doi.org/10.1016/j.neuron.2017.12.043

Tian, Y., Yang, C., Shang, S., Cai, Y., Deng, X., Zhang, J., Shao, F., Zhu, D., Liu, Y., Chen, G., Liang, J., Sun, Q., Qiu, Z., & Zhang, C. (2017). Loss of FMRP impaired hippocampal long-term plasticity and spatial learning in rats. *Frontiers in Molecular Neuroscience*, 10, 269. https://doi.org/10.3389/fnmol.2017.00269

952 Tirko, N. N., Eyring, K. W., Carcea, I., Mitre, M., Chao, M. V., Froemke, R. C., Tsien, R. W. (2018).
953 Oxytocin transforms firing mode of CA2 hippocampal neurons. *Neuron*, 100(3), 593-
954 608.e3. https://doi.org/10.1016/j.neuron.2018.09.008

955 Tsai, T.-C., Fang, Y.-S., Hung, Y.-C., Hung, L.-C., Hsu, K.-S. (2022). A dorsal CA2 to ventral CA1
956 circuit contributes to oxytocinergic modulation of long-term social recognition memory.
957 *Journal of Biomedical Science*, 29(1), 50. https://doi.org/10.1186/s12929-022-00834-x

958 Tyzio, R., Nardou, R., Ferrari, D. C., Tsintsadze, T., Shahrokhi, A., Eftekhari, S., Khalilov, I.,
959 Tsintsadze, V., Brouchoud, C., Chazal, G., Lemonnier, E., Lozovaya, N., Burnashev, N.,
960 & Ben-Ari, Y. (2014). Oxytocin-mediated GABA inhibition during delivery attenuates
961 autism pathogenesis in rodent offspring. *Science*, 343(6171), 675–679.
962 https://doi.org/10.1126/SCIENCE.1247190/SUPPL_FILE/675.MP3

963 Verkerk, A. J., Pieretti, M., Sutcliffe, J. S., Fu, Y. H., Kuhl, D. P., Pizzuti, A., ... & Warren, S. T.
964 (1991). Identification of a gene (FMR-1) containing a CGG repeat coincident with a
965 breakpoint cluster region exhibiting length variation in fragile X syndrome. Cell, 65(5), 905-
966 914.

967 Williams, T. A., Porter, M. A., & Langdon, R. (2014). Social approach and emotion recognition in
968 Fragile X Syndrome. *American Journal on Intellectual and Developmental Disabilities*,
969 119(2), 133–150. https://doi.org/10.1352/1944-7558-119.2.133

970 Wong, H., Hooper, A. W. M., Niibori, Y., Lee, S. J., Hategan, L. A., Zhang, L., Karumuthil-Melethil,
971 S., Till, S. M., Kind, P. C., Danos, O., Bruder, J. T., & Hampson, D. R. (2020). Sexually
972 dimorphic patterns in electroencephalography power spectrum and autism-related
973 behaviors in a rat model of fragile X syndrome. *Neurobiology of Disease*, 146, 105118.
974 https://doi.org/10.1016/J.NBD.2020.105118

975 Yang, M., & Crawley, J. N. (2009). Simple behavioral assessment of mouse olfaction. *Current*
976 *Protocols in Neuroscience*, 48(1), 8.24.1-8.24.12.
977 https://doi.org/10.1002/0471142301.NS0824S48

978 Zheng, C., Bieri, K. W., Hsiao, Y. T., & Colgin, L. L. (2016). Spatial sequence coding differs during
979 slow and fast gamma rhythms in the hippocampus. *Neuron*, 89(2), 398–408.
980 https://doi.org/10.1016/j.neuron.2015.12.005

981

982 **Figure Legends**

983 **Figure 1. Behavioral task.** Rats explored a 1-meter x 1-meter open field arena across four 20-
984 minute sessions per day (Sessions A, B, B', A'). A stimulus cage, which was a standard rat
985 housing cage, was placed in a corner of the arena. In the first and final sessions (A and A') of
986 both experimental conditions (i.e., Odor and Visual + Odor) and in all four sessions of the
987 Control condition, a clean cage containing clean bedding was presented. In the middle two
988 sessions (B and B') of the experimental conditions, a cage containing social stimuli was

989 presented. In the Odor condition, the soiled bedding of a familiar rat or rats served as the social
990 stimuli. In the Visual + Odor condition, a cage containing a familiar rat and the rat's soiled
991 bedding was presented.

992 **Figure 2. CA2 place cells in WT and FXS rats.** Color-coded firing rate maps are shown for all
993 place cells recorded on a single example tetrode across all conditions for WT (A) and FXS (B)
994 rats. Rate maps are shown scaled to the maximal firing rate (shown inset) of each cell across all
995 sessions. White pixels indicate places that were not visited during a session.

996 **Figure 3. CA2 place cells changed their firing fields in response to social stimuli in WT,**
997 **but not FXS, rats.** (A) The estimated means of spatial correlation coefficients from the
998 generalized linear mixed model are shown for each genotype across each condition for all
999 session pairs combined. Dots represent estimated mean values, and error bars represent the
1000 estimated 95% confidence intervals. Spatial correlation coefficients were lower in the Odor and
1001 Visual + Odor conditions compared to the Control condition for WT rats. Spatial correlation
1002 coefficients did not differ across social and control conditions in FXS rats. (B-F) Spatial
1003 correlation measures are shown for the entire sample of CA2 place cells for all pairs of sessions
1004 across all conditions. Each marker represents a spatial correlation value for an individual place
1005 cell. Different symbols are used for CA2 place cells recorded from different rats. Data from WT
1006 and FXS rats are shown with blue and red symbols, respectively.

1007 **Figure 4. Basic firing and spatial coding properties of CA2 place cells did not differ**
1008 **between WT and FXS rats.** For all plots, individual dots represent the mean value for each rat,
1009 and error bars represent 95% confidence intervals across all place cells within a rat. Data from
1010 WT rats and FXS rats are shown in blue and red, respectively. (A) Spatial information did not
1011 differ between WT and FXS rats across sessions and conditions. (B-C) CA2 place cells in FXS
1012 rats showed normal firing rates. Peak firing rates (B) and average in-field firing rates (C) of CA2
1013 place cells did not differ between WT and FXS rats across sessions and conditions. (D) CA2

1014 place field sizes were similar between genotypes and across sessions and experimental
1015 conditions. (E) The average number of place fields per place cell did not differ between
1016 genotypes across all sessions and conditions.

1017 **Figure 5. WT and FXS rats explored social stimuli similarly.** (A-B) Heat maps show mean
1018 exploration times across locations in the arena, with the stimulus cage shown in the top right
1019 corner. Exploration times were calculated for the first 2 minutes of each individual session,
1020 averaged within each rat, and then averaged across rats within each genotype group for WT (A)
1021 and FXS (B) rats. (C) Time spent exploring locations close to the cage (within 12 cm) was
1022 calculated for each session and then averaged within a rat. Individual dots represent the mean
1023 exploration time for each rat, and error bars represent 95% confidence intervals across all
1024 sessions within a rat. Exploration times are shown in blue for WT rats and in red for FXS rats.
1025 Both WT and FXS rats increased their exploration time of the stimulus cage in session B for the
1026 Odor and Visual + Odor conditions but not the Control condition.

1027 **Figure 6. FXS rats could detect and differentiate between social odors.** The normalized
1028 times spent sniffing a cotton-tip applicator is shown for trials with no odor ("null" trials, N1-N3),
1029 an initially unfamiliar social odor ("habituation" trials, H1-H4), and a second unfamiliar social
1030 odor ("dishabituation" trial, D). Bars indicate mean values within genotype and trial and dots
1031 indicate values from individual rats. Both WT (blue) and FXS (red) rats increased the time spent
1032 sniffing between null trial 3 (N3) and habituation 1 (H1), indicating that both WT and FXS rats
1033 successfully detected the presentation of a social odor. Both WT and FXS rats decreased the
1034 time spent sniffing across habituation trials (H1-4), indicating that FXS rats habituated normally
1035 to repeated presentations of the same odor. Both WT and FXS rats increased time spent
1036 sniffing between habituation trial 4 (H4) and the dishabituation trial (D), indicating that both WT
1037 and FXS rats distinguished between different social odors.

1038 **Figure 7. Low oxytocin receptor expression levels in CA2 of FXS rats.** (A-B) Example
1039 images of CA2 immunostaining in WT (A) and FXS (B) rats for a CA2 marker (Purkinje cell
1040 protein 4 (PCP4), red, top row) and an oxytocin receptor antibody (OXTR-2, green, middle row).
1041 DAPI nuclear staining is shown in blue. Merged images for PCP4 and OXTR-2 immunostaining
1042 are shown in the bottom row. Scale bar: 500 μm. (C) Plots show fluorescence estimates (mean
1043 ± 95% confidence intervals) across hippocampal subregions for WT (blue) and FXS (red) rats.
1044 Oxytocin receptor expression across subregions was lower in FXS rats than in WT rats.
1045 **Figure 8. Oxytocin depolarized the resting membrane potential in CA2 neurons in WT rats**
1046 **but not FXS rats.** Resting membrane potential (V_M) measurements are shown during baseline
1047 and after 15 minutes of 400 nM TGOT application. Dots indicate data from individual cells.
1048 TGOT significantly depolarized the V_M of WT CA2 neurons (blue; n = 6 cells from 4 rats) but not
1049 FXS CA2 neurons (red; n = 6 cells from 4 rats).
1050 **Figure S1. Histological identification of CA2.** (A) In four rats, brains were immunostained
1051 with the CA2 marker STEP (brown) and cresyl violet (purple). The boundaries of CA2 are
1052 denoted by black lines in both images. Subregions CA1, CA2, and CA3 are labeled. Right: Two
1053 example tetrode tracks are shown. The tetrode circled in red recorded place cells from CA2, and
1054 the tetrode circled in blue recorded place cells from CA3. (B) In rats in which STEP staining did
1055 not clearly differentiate the boundaries of CA2, identification of CA2 was aided by its
1056 characteristic increase in cell body size. Boundaries of CA2 are indicated by the black arrows. A
1057 CA2 tetrode track is circled in red. (C) In eight rats, brains were immunostained with CA2-
1058 expressed protein (PCP4; red) and DAPI (blue). A CA2 tetrode track is shown.
1059 **Figure S2. CA2 place cells did not significantly alter their firing rates in response to**
1060 **social stimuli in WT or FXS rats.** (A) The estimated means of rate overlap values from a
1061 generalized linear mixed model are shown for each genotype across each condition for all
1062 session pairs combined. Dots represent estimated mean values, and error bars represent the

1063 estimated 95% confidence intervals. Rate overlap values did not differ across genotypes or
1064 conditions. (B-F) Rate overlap values are shown for the entire sample of CA2 place cells for all
1065 pairs of sessions across all conditions. Each marker represents a rate overlap value for an
1066 individual place cell. Different symbols are used for CA2 place cells recorded from different rats.
1067 Values from WT and FXS rats are shown with blue and red symbols, respectively.

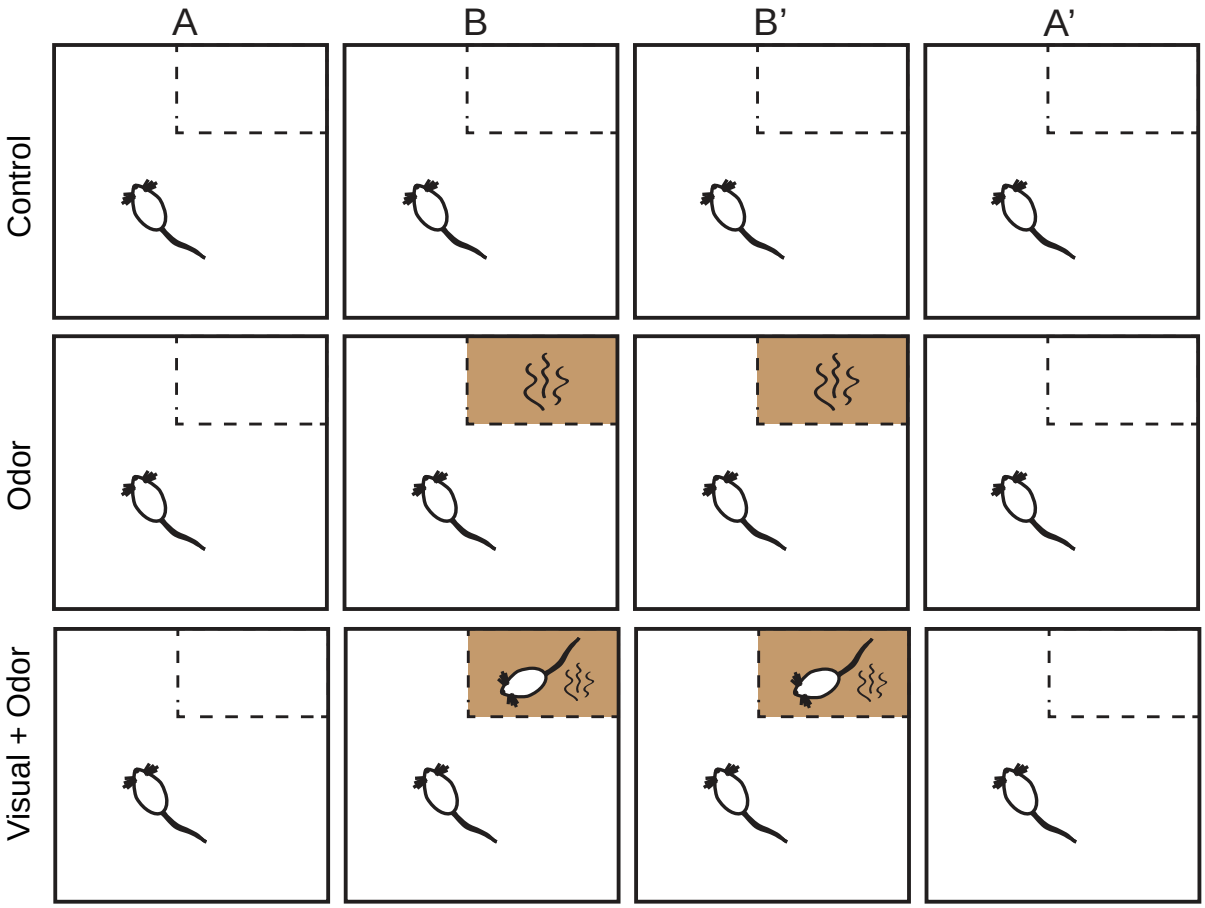

Figure 1

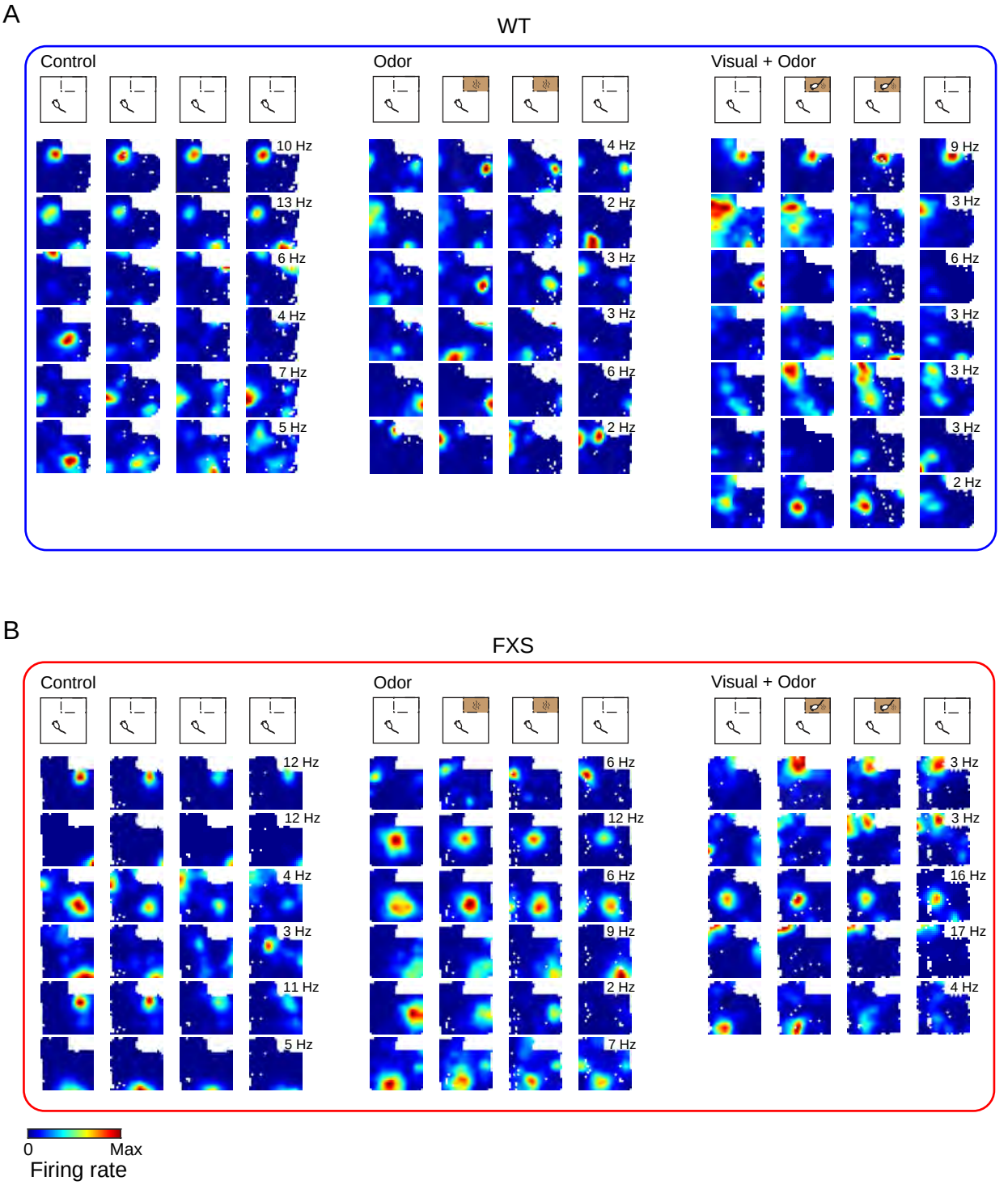
A
WT
Control
Odor
Visual + Odor
10 Hz
13 Hz
6 Hz
4 Hz
7 Hz
5 Hz
4 Hz
2 Hz
3 Hz
3 Hz
6 Hz
2 Hz
9 Hz
3 Hz
6 Hz
3 Hz
3 Hz
3 Hz
2 Hz
B
FXS
Control
Odor
Visual + Odor
12 Hz
12 Hz
4 Hz
3 Hz
11 Hz
5 Hz
6 Hz
12 Hz
6 Hz
9 Hz
2 Hz
7 Hz
3 Hz
3 Hz
16 Hz
17 Hz
4 Hz
0
Max
Firing rate

Figure 2

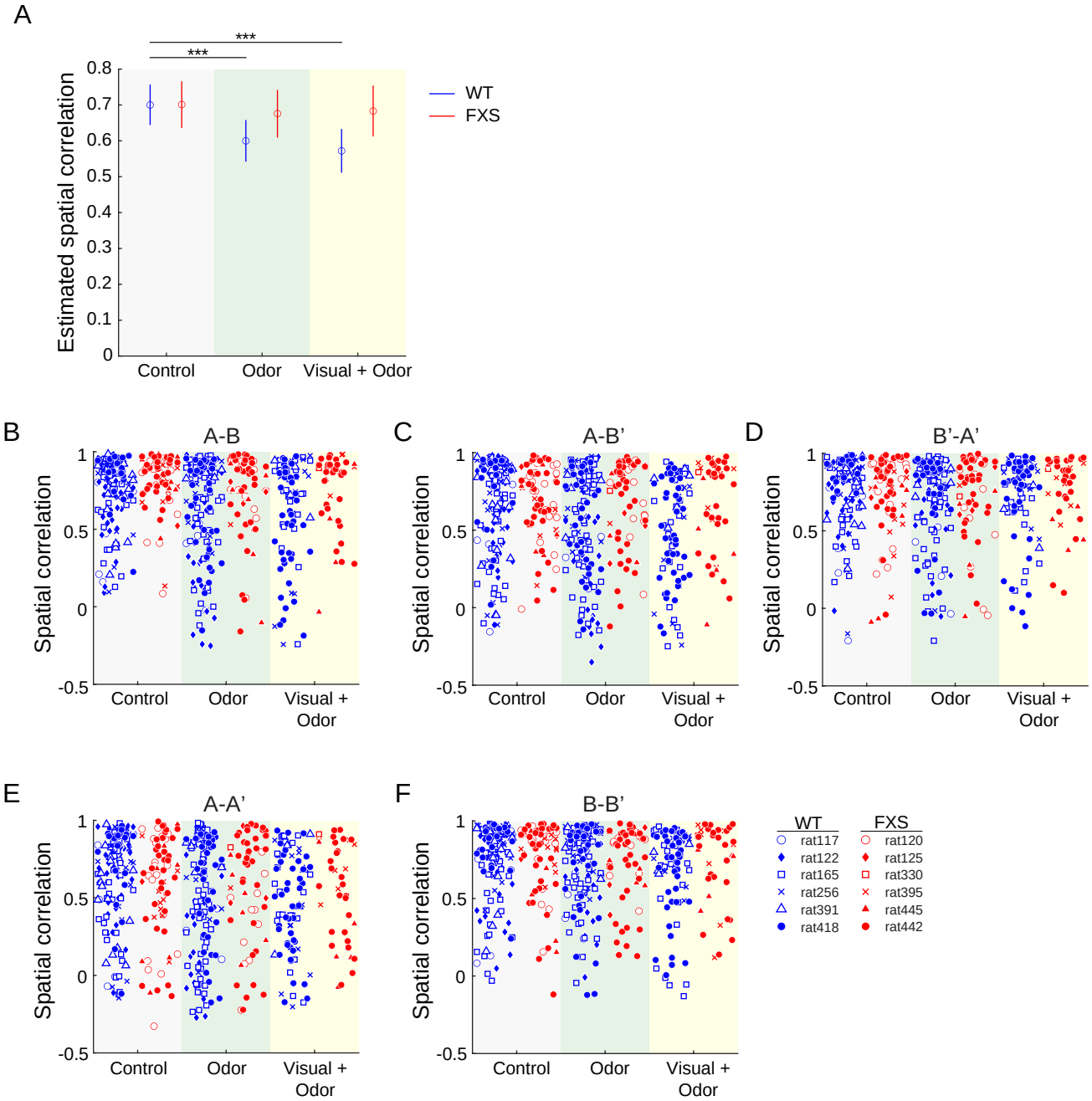
A
***
***
Estimated spatial correlation
0.8
0.7
0.6
0.5
0.4
0.3
0.2
0.1
0
Control
Odor
Visual + Odor
WT
FXS
B
A-B
C
A-B'
D
B'-A'
E
A-A'
F
B-B'
Spatial correlation
1
0.5
0
-0.5
Control
Odor
Visual + Odor
WT
rat117
rat122
rat165
rat256
rat391
rat418
FXS
rat120
rat125
rat330
rat395
rat445
rat442

Figure 3

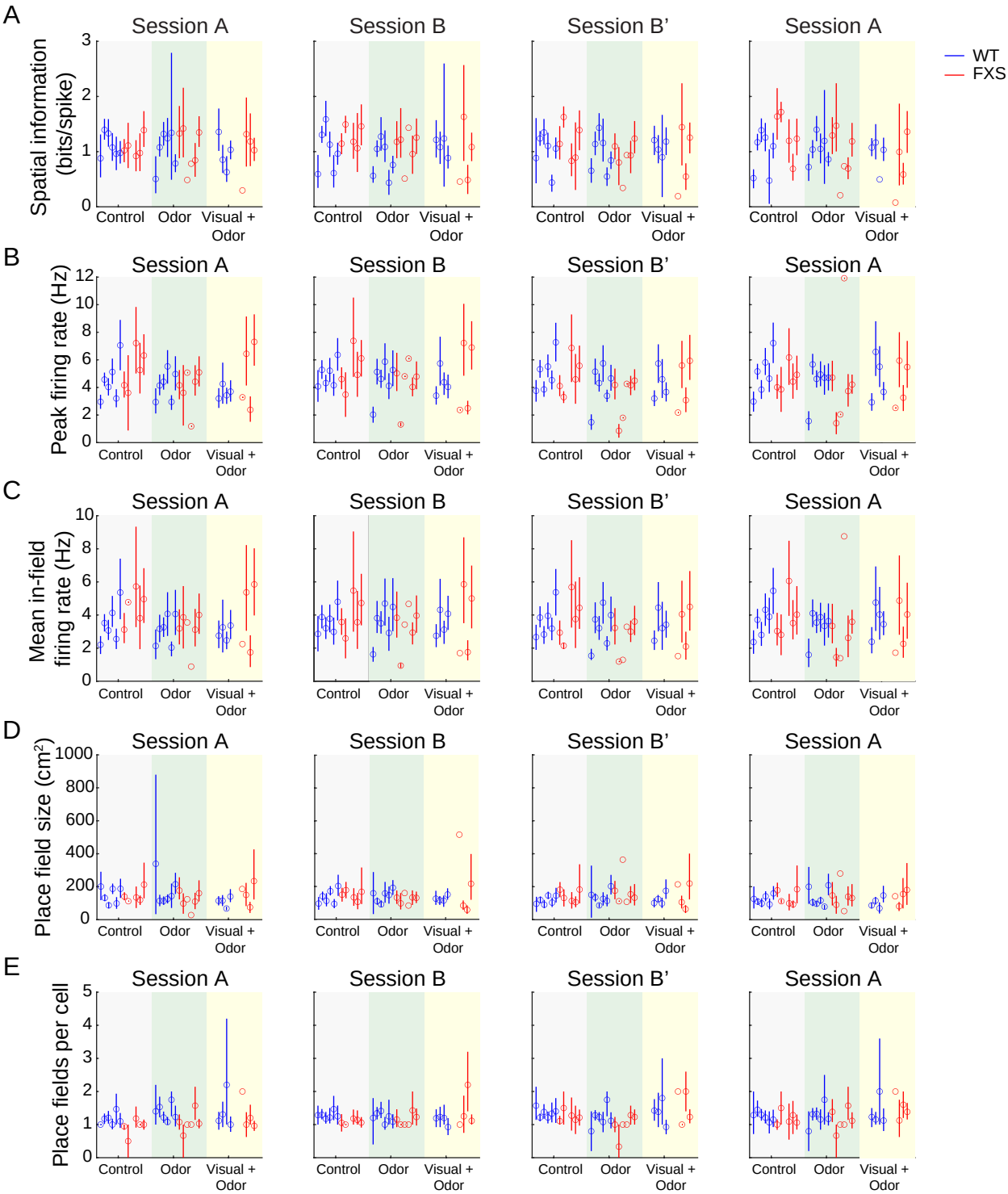
A
Session A
Session B
Session B'
Session A
WT
FXS
Spatial information (bits/spike)
Control
Odor
Visual + Odor
B
Peak firing rate (Hz)
C
Mean in-field firing rate (Hz)
D
Place field size (cm²)
E
Place fields per cell

Figure 4

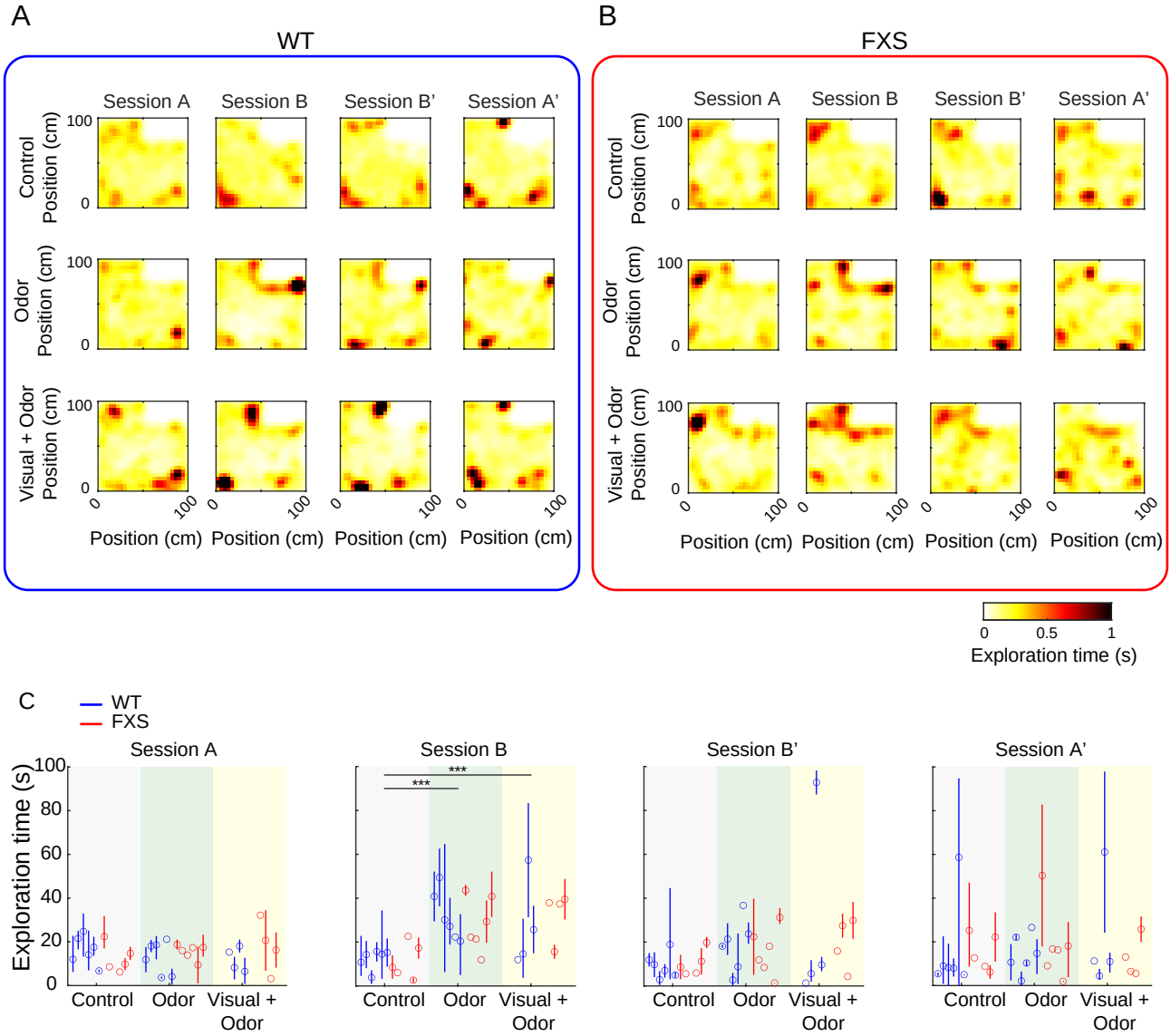
A
WT
Session A
Session B
Session B'
Session A'
Control Position (cm)
Odor Position (cm)
Visual + Odor Position (cm)
100
0
Position (cm)
B
FXS
0
0.5
1
Exploration time (s)
C
WT
FXS
Exploration time (s)
Control
Odor
Visual + Odor
***

Figure 5

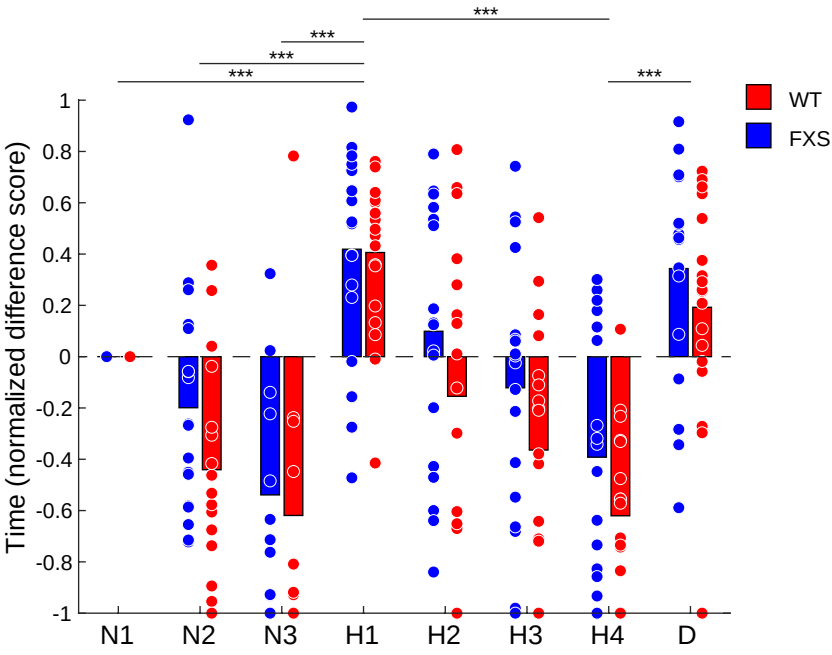
***
***
***
***
***
WT
FXS
Time (normalized difference score)
1
0.8
0.6
0.4
0.2
0
-0.2
-0.4
-0.6
-0.8
-1
N1
N2
N3
H1
H2
H3
H4
D

Figure 6

A

WT

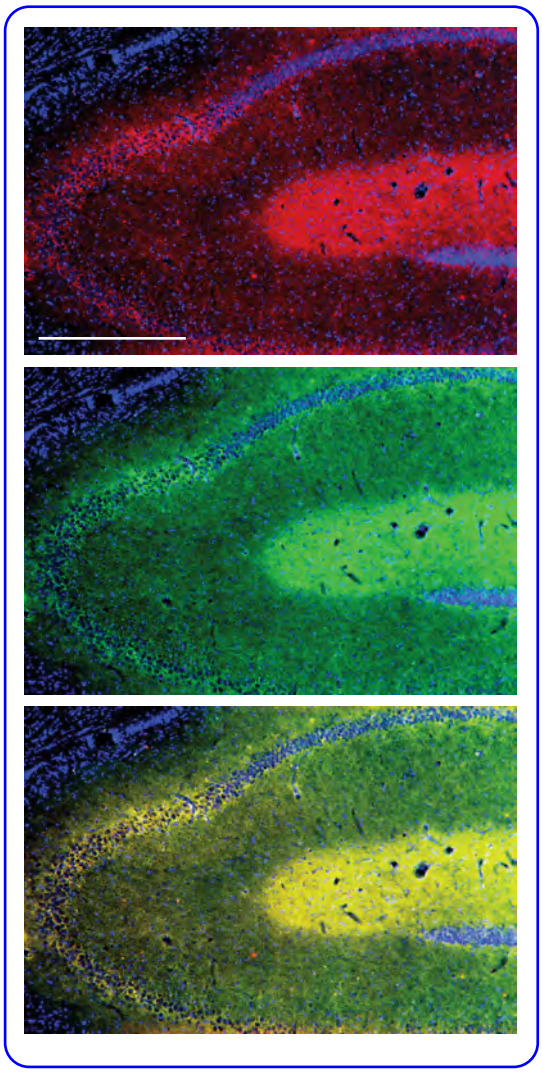

B

FXS

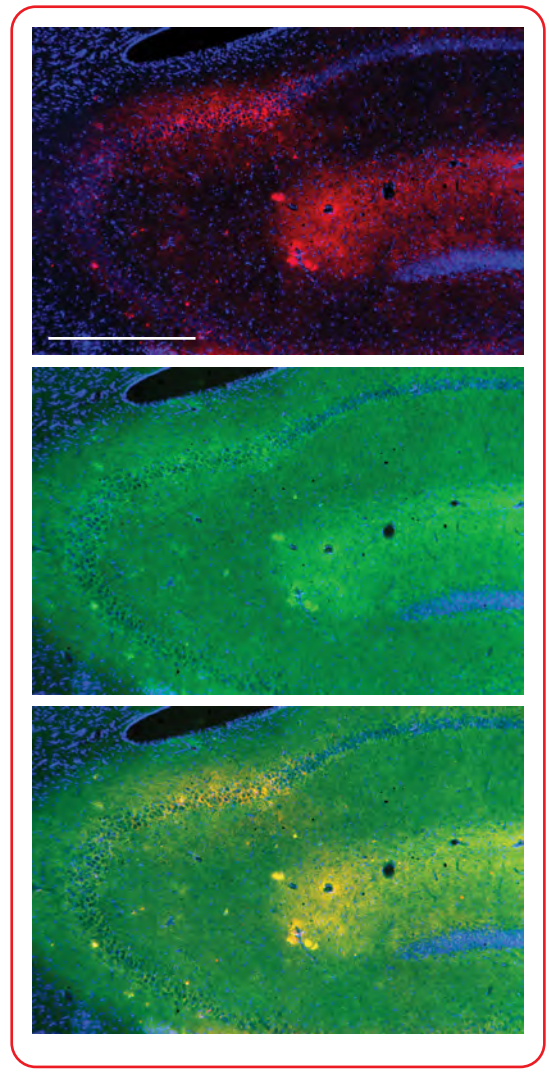

C

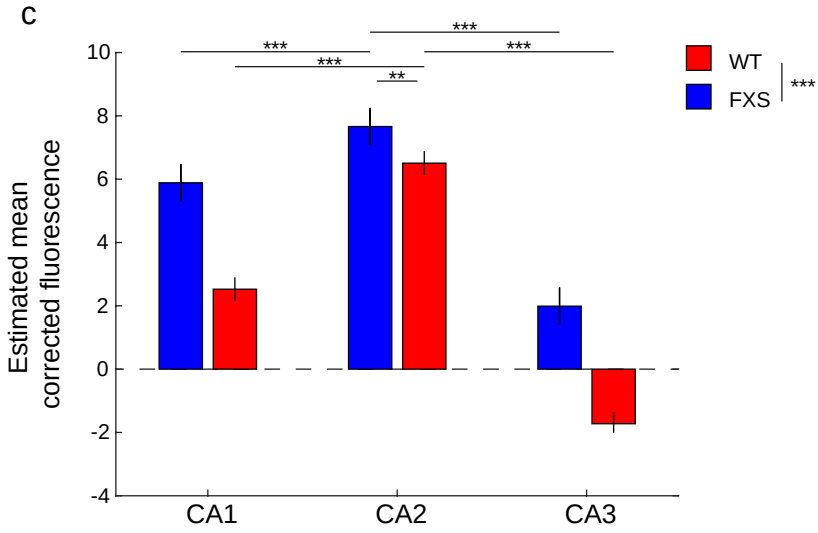

Figure 7

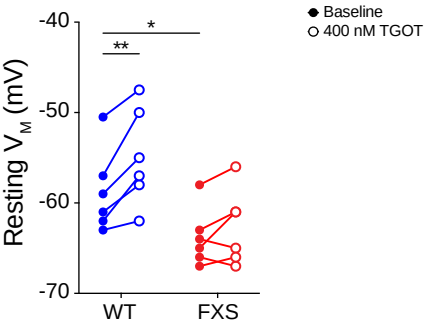

Figure 8

A

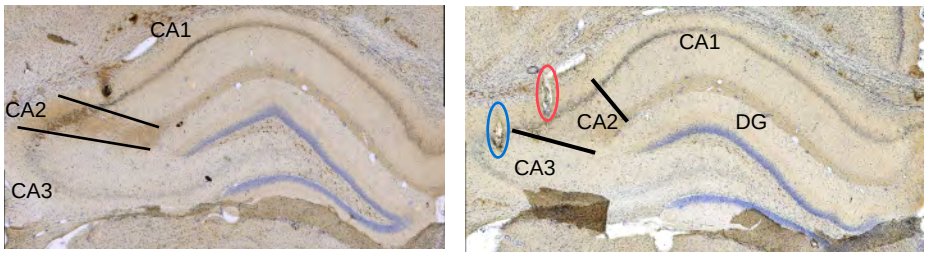

B

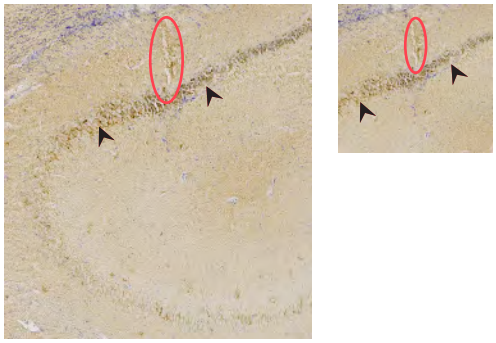

C

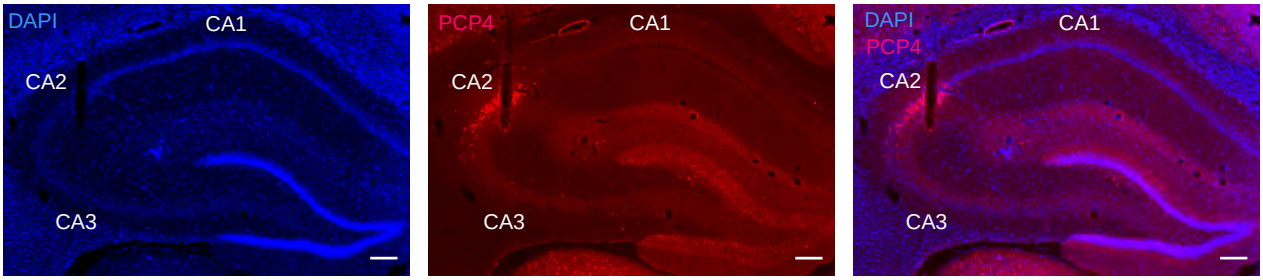

Figure S1

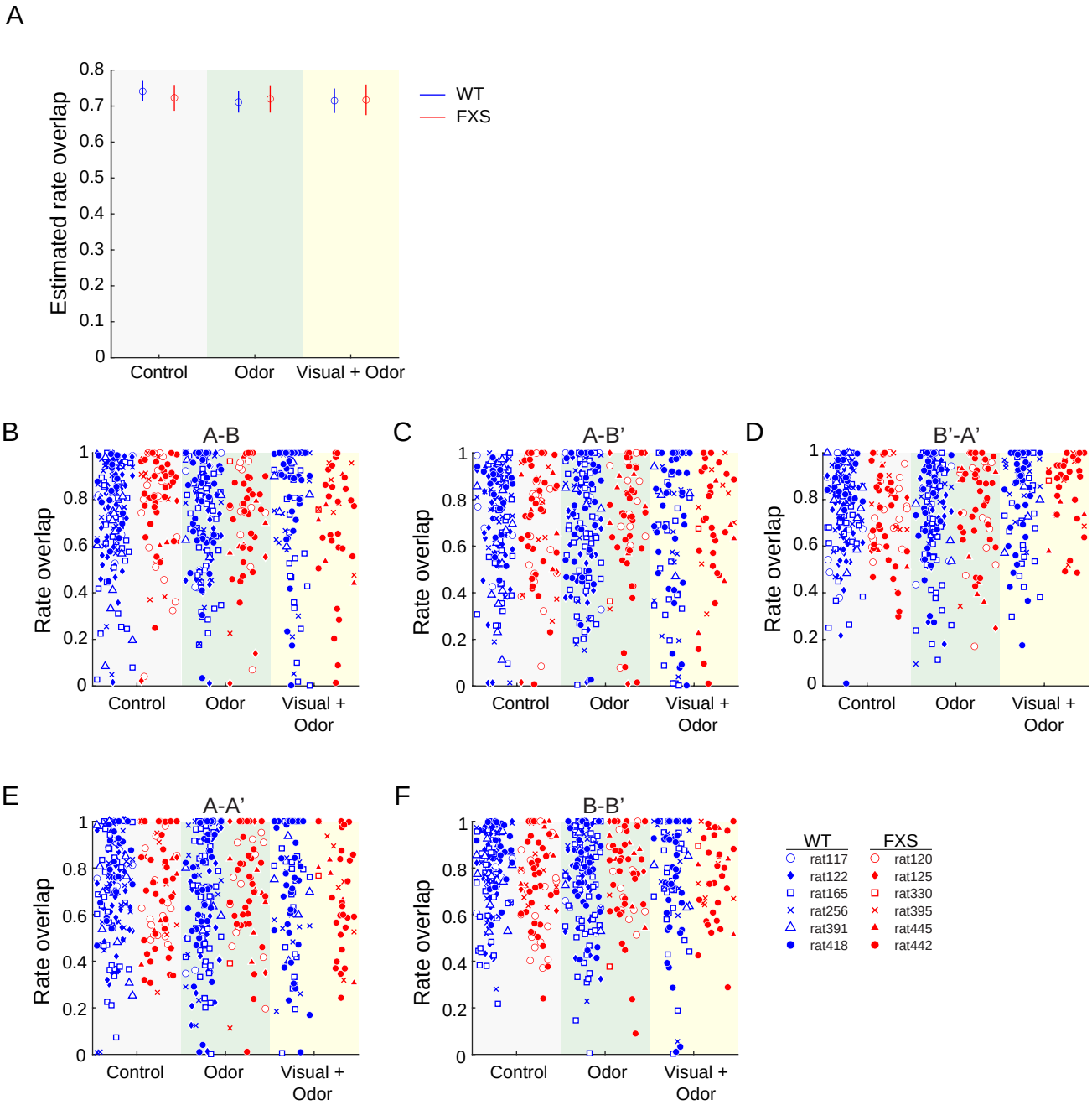
A
Estimated rate overlap
0.8
0.7
0.6
0.5
0.4
0.3
0.2
0.1
0
Control
Odor
Visual + Odor
WT
FXS
B
A-B
C
A-B'
D
B'-A'
E
A-A'
F
B-B'
Rate overlap
1
0.8
0.6
0.4
0.2
0
Control
Odor
Visual + Odor
WT
rat117
rat122
rat165
rat256
rat391
rat418
FXS
rat120
rat125
rat330
rat395
rat445
rat442

Figure S2